

---

# AutoStep: Locally adaptive involutive MCMC

---

Tiange Liu

University of British Columbia

Nikola Surjanovic

University of British Columbia

Miguel Biron-Lattes

University of British Columbia

Alexandre Bouchard-Côté

University of British Columbia

Trevor Campbell

University of British Columbia

## Abstract

Many common Markov chain Monte Carlo (MCMC) kernels can be formulated using a deterministic involutive proposal with a step size parameter. Selecting an appropriate step size is often a challenging task in practice; and for complex multiscale targets, there may not be one choice of step size that works well globally. In this work, we address this problem with a novel class of involutive MCMC methods—AutoStep MCMC—that selects an appropriate step size at each iteration adapted to the local geometry of the target distribution. We prove that AutoStep MCMC is  $\pi$ -invariant and has other desirable properties under mild assumptions on the target distribution  $\pi$  and involutive proposal. Empirical results examine the effect of various step size selection design choices, and show that AutoStep MCMC is competitive with state-of-the-art methods in terms of effective sample size per unit cost on a range of challenging target distributions.

## 1 INTRODUCTION

Markov chain Monte Carlo (MCMC) (Metropolis et al., 1953; Hastings, 1970) is an effective tool for approximating integrals arising in Bayesian inference problems. The performance of MCMC is often sensitive to the choice of tuning parameters in the Markov kernel. In particular, methods that propose a new state followed by an accept/reject step—e.g., random-walk Metropolis–Hastings (RWMH) (Hastings, 1970), the Metropolis-adjusted Langevin algorithm (MALA)

(Rosky et al., 1978), and Hamiltonian Monte Carlo (HMC) (Duane et al., 1987; Neal, 1996)—often involve a scalar *step size* parameter  $\theta \geq 0$  that governs the distance of the proposed next state from the current state. Too large a choice of  $\theta$  results in distant proposals that are often rejected, while too small a choice leads to nearby proposals that do not explore the state space quickly; either case results in slow convergence of the chain. For certain multiscale targets (e.g. Bayesian posteriors with scale priors (Polson and Scott, 2012)) there may not even be a single good choice of step size throughout the whole state space.

Existing methods for selecting step size parameters fall generally into three categories: adaptive MCMC, discrepancy minimization, and locally-adaptive kernels. Adaptive MCMC algorithms (Haario et al., 2001; Atchadé, 2006; Andrieu and Thoms, 2008; Marshall and Roberts, 2012) tune the proposal distribution using previous draws from the chain, often targeting a particular acceptance rate derived from high-dimensional asymptotics (Roberts et al., 1997; Roberts and Rosenthal, 1998). Obtaining theoretical guarantees on estimates produced by adaptive MCMC targeting a distribution  $\pi$  is technically difficult and often requires strict conditions on the adaptation process, such as increasingly infrequent adaptation (Chimisov et al., 2018). Discrepancy minimization (Neklyudov et al., 2018; Coullon et al., 2023) involves tuning using a divergence between the empirical distribution of draws and the target  $\pi$ , which requires multiple MCMC runs to estimate the divergence for each candidate step size. Both approaches also identify only a single step size value, which may not be appropriate for the whole state space.

Locally-adaptive kernels, in contrast, select a value for the step size *at each iteration* based on the current state. Because the step size depends on the current state, these kernels can adapt to the local shape of the target  $\pi$ ; and because they depend only on the current state, they are Markovian and one can use standard tools to prove  $\pi$ -invariance. There are many approaches to locally adaptive step size selection in the literature.

---

The code, data, and instructions needed to reproduce the main experimental results:

<https://github.com/Julia-Tempering/soft-auto-mev>

Mixture kernels with state-dependent weights (Maire and Vandekerckhove, 2022) and delayed-rejection (Tierney and Mira, 1999; Green and Mira, 2001) are both general approaches, but each requires a prespecified maximum number of step sizes to consider at each iteration. There are also numerous methods specific to certain samplers, e.g., HMC and MALA (Girolami and Calderhead, 2011; Nishimura and Dunson, 2016; Kleppe, 2016; Modi et al., 2023; Biron-Lattes et al., 2024; Turok et al., 2024), RWMH (see Livingstone, 2021), or slice sampling (Neal, 2003). Of these, the method most related to the present work is autoMALA (Biron-Lattes et al., 2024), which chooses a step size in MALA using a doubling/halving procedure that targets a Metropolis–Hastings acceptance ratio in a randomized range  $(a, b) \subset [0, 1]$ . While the method was shown to be  $\pi$ -invariant, it includes a hard reversibility check that can prevent the chain from moving in challenging areas of the state space. Furthermore, important theoretical properties beyond invariance—especially irreducibility and aperiodicity—were not demonstrated.

In this work, we develop a method for locally-adaptive step size selection in the broad class of involutive MCMC methods (Tierney, 1998; Andrieu et al., 2020; Neklyudov et al., 2020). We show that these Markov kernels are  $\pi$ -invariant, irreducible, and aperiodic under mild assumptions on the target distribution, and investigate bounds on energy jump distances. Empirical results demonstrate that the step size selection method performs well across a wide range of examples. Proofs of all theoretical results are provided in Appendix A.

## 2 BACKGROUND

Let  $\pi$  be a given target probability distribution on an open subset  $\mathcal{X} \subset \mathbb{R}^d$ . With a slight abuse of notation, we assume that  $\pi$  admits a density  $\pi(x)$  with respect to the Lebesgue measure on  $\mathbb{R}^d$ , and that we can evaluate a function  $\gamma(x) \propto \pi(x)$  pointwise so that

$$\pi(x) = \frac{\gamma(x)}{\int \gamma(x) dx},$$

where  $\int \gamma(x) dx$  is the unknown normalizing constant.

Involutive Markov Chain Monte Carlo (Tierney, 1998; Andrieu et al., 2020; Neklyudov et al., 2020) is an MCMC method that uses *involutions*, i.e., functions  $f$  where  $f^{-1} = f$ , to generate new proposals. While there are many possible variations of involutive MCMC, in this work we use the following formulation. Fix a distribution  $m$  on an open subset  $\mathcal{Z} \subset \mathbb{R}^p$  with density  $m(z)$  with respect to the Lebesgue measure, and a family of differentiable involutions  $f_\theta : \mathcal{X} \times \mathcal{Z} \rightarrow \mathcal{X} \times \mathcal{Z}$  parametrized by  $\theta \in \Theta$ . Then, starting from a state  $x_t$ ,

we draw  $z_t \sim m$  and the proposal

$$x'_{t+1}, z'_{t+1} = f_\theta(x_t, z_t). \quad (1)$$

We set the next state to  $x_{t+1} = x'_{t+1}$  with probability

$$\min\{1, \exp(\ell(x_t, z_t, \theta))\}, \quad (2)$$

where

$$\ell(x_t, z_t, \theta) = \log \left( \frac{\pi(x'_{t+1})m(z'_{t+1})}{\pi(x_t)m(z_t)} |\nabla f_\theta(x_t, z_t)| \right),$$

and otherwise set it to  $x_{t+1} = x_t$ . The sequence  $x_t$  is a Markov chain and has stationary distribution  $\pi$  if  $f_\theta$  is continuously differentiable (Tierney, 1998, Thm. 2).

Choosing different families of involutions  $\{f_\theta\}$  and auxiliary distributions  $m$  yields different MCMC algorithms. For example, random walk Metropolis–Hastings (RWMH) (Hastings, 1970) with step size  $\theta > 0$  and mass matrix  $M$  is obtained by setting

$$f_\theta(x, z) = (x + \theta z, -z) \quad m = \mathcal{N}(0, M).$$

The Metropolis-adjusted Langevin algorithm (MALA) (Rosky et al., 1978) with step size  $\theta > 0$  and mass matrix  $M$  is obtained by setting

$$f_\theta(x, z) = (x', -z') \quad m = \mathcal{N}(0, M),$$

where  $x', z'$  are computed via the *leapfrog* map

$$\begin{aligned} z_{1/2} &\leftarrow z + \frac{\theta}{2} \nabla \log \pi(x) \\ x' &\leftarrow x + \theta M^{-1} z_{1/2} \\ z' &\leftarrow z_{1/2} + \frac{\theta}{2} \nabla \log \pi(x'). \end{aligned}$$

Finally, Hamiltonian Monte Carlo (HMC) (Duane et al., 1987; Neal, 1996) with step size  $\theta > 0$ , mass matrix  $M$ , and path length  $L$  is obtained by setting

$$f_\theta(x, z) = (x', -z') \quad m = \mathcal{N}(0, M),$$

where  $x', z'$  are computed via  $L$  leapfrogs.

Many involutive MCMC methods—including the above three examples—have a positive scalar tuning parameter  $\theta > 0$  that can be interpreted as a form of “step size”: larger values result in more distant proposals, while smaller values result in nearby proposals. Too large a choice of  $\theta$  results in many rejected proposals, while too small a choice results in proposals that are accepted but explore the state space slowly. Furthermore, there may not be a single choice of  $\theta$  that applies globally, e.g., in the case of multiscale targets (Polson and Scott, 2012). This work resolves this problem by selecting an appropriate  $\theta$  at each iteration depending on the local behaviour of the augmented target  $\pi \cdot m$ .

---

**Algorithm 1** One iteration of AutoStep MCMC

---

**Require:** Initial value  $x$  with  $\pi(x) > 0$ , target  $\pi$ , auxiliary distribution  $m$ , step size distribution  $\eta$ , involutions  $\{f_\theta\}_{\theta \in \Theta}$

- 1:  $z \sim m$  ▷ auxiliary refreshment
  - 2:  $(a, b) \sim \text{Unif}(\Delta)$  ▷ soft acceptance bounds
  - 3:  $\theta \sim \eta(d\theta \mid x, z, a, b)$  ▷ refresh tuning parameter
  - 4:  $s \leftarrow (x, z, a, b, \theta)$  ▷ augmented state
  - 5:  $s' \leftarrow \bar{f}(s)$  ▷ involutive proposal
  - 6:  $U \sim \text{Unif}[0, 1]$
  - 7: **if**  $U \leq \min\left\{1, \frac{\bar{\pi}(s')}{\bar{\pi}(s)} J(s)\right\}$  **then**
  - 8:     **return**  $x'$  ▷ accept
  - 9: **else**
  - 10:     **return**  $x$  ▷ reject
  - 11: **end if**
- 

### 3 AUTOSTEP MCMC

In this section, we develop *AutoStep MCMC*, a family of modified involutive MCMC methods that automatically select appropriate tuning parameter values at each iteration. The key technique in developing AutoStep MCMC is to formulate the sampler on an augmented space that includes the tuning parameter  $\theta \in \Theta$  as well as other auxiliary quantities. For a given family of continuously differentiable involutions  $\{f_\theta : \theta \in \Theta\}$  on  $\mathcal{X} \times \mathcal{Z}$ , define the augmented state space  $\mathcal{S}$  as

$$\mathcal{S} = \mathcal{X} \times \mathcal{Z} \times \Delta \times \Theta,$$

where  $\mathcal{X} \times \mathcal{Z}$  is the original augmented space for involutive MCMC,  $\Delta := \{a, b \in (0, 1)^2 : a < b\}$  is a set of acceptance ratio thresholds  $(a, b)$ , and  $\Theta$  is the set of tuning parameters  $\theta$  for the involutions. We assume  $\Theta$  is a standard Borel space, such that  $\mathcal{S}$  is standard Borel as well. Let  $\bar{f} : \mathcal{S} \rightarrow \mathcal{S}$  denote the augmented involution  $f_\theta$ : for a point  $s = (x, z, a, b, \theta) \in \mathcal{S}$ , define

$$\bar{f}(s) = (f_\theta(x, z), a, b, \theta) \quad J(s) = |\nabla f_\theta(x, z)|.$$

Note that  $\bar{f}$  is itself an involution on  $\mathcal{S}$ . We then define the augmented target density

$$\bar{\pi}(s) = 2\pi(x) \cdot m(z) \cdot \mathbf{1}_\Delta(a, b) \cdot \eta(\theta \mid x, z, a, b),$$

where we assume that  $\pi(x)$  and  $m(z)$  are with respect to the Lebesgue measure on  $\mathcal{X} \times \mathcal{Z}$ , that both  $m$  and  $\eta$  admit i.i.d. draws, and that there exists a  $\sigma$ -finite measure  $d\theta$  on  $\Theta$  such that for all  $x \in \mathcal{X}$ ,  $z \in \mathcal{Z}$  and  $(a, b) \in \Delta$ ,  $\eta(\cdot \mid x, z, a, b)$  is a density with respect to  $d\theta$ , but otherwise may depend arbitrarily on  $x, z, a, b$ . The  $\mathcal{X}$ -marginal of  $\bar{\pi}$  is the target of interest,  $\pi$ . See concurrent work of Bou-Rabee et al. (2024b) and Bou-Rabee et al. (2024a) for a related augmentation.

Given this setup, starting from  $x_t \in \mathcal{X}$ , AutoStep MCMC (Algorithm 1) consists of the following steps:

1. **Auxiliary refreshment:** Draw

$$z_t \sim m \quad \text{and} \quad (a_t, b_t) \sim \text{Unif}(\Delta).$$

2. **Tuning parameter refreshment:** Draw

$$\theta_t \sim \eta(d\theta \mid x_t, z_t, a_t, b_t).$$

3. **Proposal:** Set  $s_t = (x_t, z_t, a_t, b_t, \theta_t)$  and

$$s'_{t+1} = \bar{f}(s_t) = (x'_{t+1}, z'_{t+1}, a'_{t+1}, b'_{t+1}, \theta'_{t+1}).$$

4. **Accept:** Set  $x_{t+1} = x'_{t+1}$  with probability

$$\min\left\{1, \frac{\bar{\pi}(s'_{t+1})}{\bar{\pi}(s_t)} J(s_t)\right\},$$

and otherwise set  $x_{t+1} = x_t$ .

We can recover standard involutive MCMC by setting  $\eta(d\theta \mid x, z, a, b) = \delta_{\theta_0}(d\theta)$  for some fixed  $\theta_0 \in \Theta$ . Further, choosing different involution families  $\{f_\theta : \theta \in \Theta\}$  and auxiliary distributions  $m$  on  $\mathcal{Z}$  recovers variants of common algorithms, e.g., RWMH, MALA, and HMC. The major improvement is that the chain may draw the tuning parameter  $\theta \in \Theta$  automatically at each step in a manner that depends on the current state  $(x_t, z_t, a_t, b_t)$ . The key design choice, then, is to select a conditional tuning refreshment distribution  $\eta$  that yields values of  $\theta$  that are well-adapted to the local shape of the target  $\bar{\pi}$ . In this work, we focus on the design of the conditional tuning refreshment distribution  $\eta$  in the case where  $\theta$  is a step size parameter (with  $\Theta = \mathbb{R}_+$ ). However, the AutoStep MCMC method described previously has the correct stationary distribution for more general parameter spaces  $\Theta$  (see Proposition 4.2).

#### 3.1 Step size selection

We now focus on the design of the tuning refreshment distribution  $\eta$  when  $\theta$  is a step size parameter with  $\Theta = \mathbb{R}_+$ . Intuitively, a good choice of  $\theta$  should yield a proposal for which the acceptance ratio  $\exp(\ell(x, z, \theta))$  of the original involutive method is not too close to either 0 ( $\theta$  is too large) or 1 ( $\theta$  is too small). Critically, this should also be true for  $\exp(-\ell(x, z, \theta))$ , which is the acceptance ratio in the reverse direction

$$\ell(f_\theta(x, z), \theta) = -\ell(x, z, \theta).$$

To avoid setting arbitrary fixed bounds on  $\ell$ , we use the random  $a, b$  as thresholds and ensure that  $|\ell|$  roughly tries to fall in the range  $(|\log(b)|, |\log(a)|)$ . We also randomize (or *jitter*) the step size  $\theta$  to avoid potentially fragile deterministic choices.

More precisely, given a fixed initial step size  $\theta_0 > 0$  and jitter variance  $\sigma^2 \geq 0$ , we propose simulating the

---

**Algorithm 2** Step size selector  $\mu$ 


---

**Require:** state  $x, z, a, b$ , initial step size  $\theta_0$ .

```

1:  $\theta \leftarrow \theta_0$ 
2:  $\ell \leftarrow \ell(x, z, \theta)$ 
3:  $v \leftarrow \mathbb{1}\{|\ell| < |\log b|\} - \mathbb{1}\{|\ell| > |\log a|\}$ 
4:  $j = 0$  ▷ number of doublings/halvings
5: if  $v = 0$  then
6:   return  $j$ 
7: end if
8: while true do
9:    $j \leftarrow j + v$ 
10:   $\theta \leftarrow \theta_0 \cdot 2^j$ 
11:   $\ell \leftarrow \ell(x, z, \theta)$ 
12:  if  $v = 1$  and  $|\ell| \geq |\log b|$  then
13:    return  $j - 1$  ▷ Require final halving
14:  else if  $v = -1$  and  $|\ell| \leq |\log a|$  then
15:    return  $j$ 
16:  end if
17: end while

```

---

step size  $\theta$  from the following conditional refreshment distribution  $\eta(d\theta|x, z, a, b)$ :

$$\delta \sim \mathcal{N}(\mu(x, z, a, b), \sigma^2) \quad \theta = \theta_0 \times 2^\delta, \quad (3)$$

where  $\mu$  is the step size selector function

$$\mu(x, z, a, b) = \begin{cases} \min\{j \in \mathbb{Z}^+ : |\ell(x, z, \theta_0 2^j)| \geq |\log b|\} - 1, & |\ell_0| < |\log b| \\ \max\{j \in \mathbb{Z}^- : |\ell(x, z, \theta_0 2^j)| \leq |\log a|\}, & |\ell_0| > |\log a| \\ 0, & \text{otherwise,} \end{cases}$$

and  $\ell_0 = \ell(x, z, \theta_0)$ . Therefore, when  $\sigma^2 > 0$ ,  $\eta(\theta|x, z, a, b)$  is a density with respect to the Lebesgue measure on  $\mathbb{R}_+$ ; but we also allow  $\sigma^2 = 0$ , which formally indicates that  $\delta = \mu(x, z, a, b)$  almost surely, in which case  $\eta(\theta|x, z, a, b)$  is a density with respect to the counting measure on  $\{\theta_0 \times 2^j : j \in \mathbb{Z}\}$ .

The pseudocode for computing  $\mu(x, z, a, b)$  is given in Algorithm 2. If the initial step size  $\theta_0$  yields an acceptable  $|\ell_0|$ , the function simply returns  $j = 0$ . If the initial step size is too large ( $|\ell_0| > |\log a|$ ),  $j$  is decreased until  $|\ell_0| \leq |\log a|$ . And if the initial step size is too small ( $|\ell_0| < |\log b|$ ),  $j$  is increased until  $|\ell_0| > |\log b|$ , and then finally decreased by 1 to avoid poor proposals. Note that this function does not guarantee that  $|\log b| \leq |\ell| \leq |\log a|$  precisely, but finds a good trade-off by approximately targeting that range while avoiding the need for expensive methods to find values exactly within the bounds.

The step size refreshment was inspired by that of autoMALA (Biron-Lattes et al., 2024), but has two important differences. First, we use symmetric thresholds that check  $|\log b| \leq |\ell| \leq |\log a|$ , instead of checking  $\log b \leq \ell \leq \log a$ . This is crucial for ensuring irreducibility of the method (see Section 4), and enables

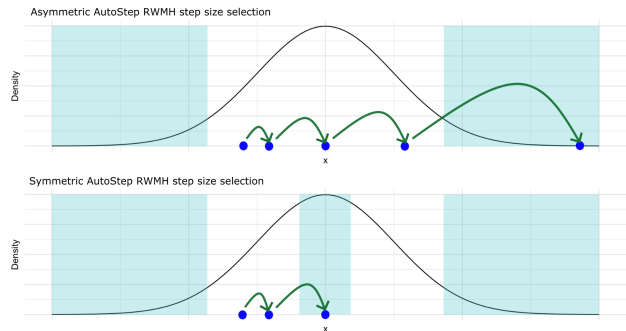


Figure 1: Symmetric acceptance thresholds help the sampler explore modal regions. Here, autostep RWMH starts at the leftmost dot and proposes moving to the right. The shaded area indicates the region where the step size selector stops doubling. If one uses asymmetric thresholds (top row) (Biron-Lattes et al., 2024), since  $\ell > \log b$ , AutoStep RWMH continues doubling the step size until  $\ell < \log(b)$ , which often leads to overshooting the mode. Our proposed symmetric thresholds (bottom row) based on  $|\ell|$  double the step size until  $|\ell| < |\log(b)|$ , enabling termination at higher density values.

the sampler to effectively visit higher density regions (see Figure 1 for an illustration). Second, we include the step size  $\theta$  as an augmentation of our state variable, which simplifies theoretical analyses (compare the proof of Proposition 4.2 in Appendix A with the proof of Theorem 3.4 in Biron-Lattes et al. (2024)) and allows for randomized step size proposals that avoid the hard reversibility checks of autoMALA.

### 3.2 Round-based tuning

The AutoStep MCMC method has two free parameters: the initial step size  $\theta_0$  and the step size jitter  $\sigma^2$ . While the method should be somewhat insensitive to  $\theta_0$  and small values of  $\sigma^2$ , it is still helpful to tune these parameters to minimize the number of doubling/halving steps. Furthermore, many involutive MCMC methods—e.g., RWMH, MALA, and HMC—have a preconditioner, or *mass matrix*  $M$  that needs to be tuned.

In this work, we use a round-based procedure to tune  $\theta_0$ ,  $\sigma^2$ , and  $M$  (Algorithm 3). Each round corresponds to a block of iterations during which these three parameters are held constant. We use  $\theta_0 = 1$ ,  $M = I$ , and  $\sigma = 0.5$  for the first round. At the end of each round, we use: (1) the average selected step size  $\theta_0 2^{\mu(x, z, a, b)}$  from the current round as the new  $\theta_0$ ; (2) the inverse of a geometric mix of the diagonal of the sample covariance matrix and the identity for  $M$ ; and (3) half the mean absolute difference  $d = |\mu(x', z', a, b) - \mu(x, z, a, b)|$  of the forward and reverse step size selections for  $\sigma$ , which controls the ratio of step size proposals  $\frac{\eta(\theta|x', z', a, b)}{\eta(\theta|x, z, a, b)}$ .

---

**Algorithm 3** Round-based AutoStep MCMC

---

**Require:** Initial state  $x_0$ , number of rounds  $R$ , target  $\pi$ , auxiliary distribution  $m$ , step size distribution  $\eta$ , involutions  $\{f_\theta\}_{\theta \in \Theta}$ .

- 1:  $\theta_0 \leftarrow 1$
- 2:  $m \leftarrow \mathcal{N}(0, I_d)$
- 3:  $\sigma \leftarrow 0.5$
- 4: **for**  $r$  **in**  $1, 2, \dots, R$  **do**
- 5:      $T \leftarrow 2^r$                       $\triangleright$  Number of iterations
- 6:      $\eta \leftarrow$  (Eq. (3)) based on  $(\theta_0, \sigma)$
- 7:     **for**  $t$  **in**  $1, 2, \dots, T$  **do**
- 8:          $\xi \sim \frac{1}{3}\delta_0 + \frac{1}{3}\delta_1 + \frac{1}{3}\text{Beta}(1, 1)$   
            $\triangleright$  Random mixing of the preconditioner
- 9:          $\widehat{\Sigma}_{i,i}^{-1/2} \leftarrow \xi \Sigma_{i,i}^{-1/2} + (1 - \xi)$
- 10:         $m \leftarrow \mathcal{N}(0, \widehat{\Sigma}^{-1})$   
            $\triangleright$  see definition of  $d_t, \mu_t$  in Section 3.2
- 11:         $x_t, \mu_t, d_t \leftarrow \text{AutoStep}(x_0, \pi, m, \eta, \{f_\theta\}_{\theta \in \Theta})$
- 12:     **end for**
- 13:      $\theta_0 \leftarrow \theta_0 T^{-1} \sum_{t=1}^T 2^{\mu_t}$
- 14:      $\sigma \leftarrow 0.5 T^{-1} \sum_{t=1}^T d_t$
- 15:      $x_0 \leftarrow x_T$
- 16:      $\Sigma \leftarrow \text{diag} \left( \left[ \widehat{\text{Var}}[x_t^{(j)}]_{t=1}^T \right]_{j=1}^d \right)$
- 17: **end for**
- 18: **return**  $\{x_t\}_{t=1}^T$

---

## 4 THEORETICAL ANALYSIS

The marginal sequence  $x_t$  on  $\mathcal{X}$  of AutoStep MCMC is itself a Markov chain because each step redraws  $z_t, a_t, b_t, \theta_t$  independently of their previous value conditioned on  $x_t$ . In this section we establish various properties of the  $\mathcal{X}$ -marginal Markov chain.

### 4.1 Invariance

First, we show that AutoStep MCMC is  $\bar{\pi}$ -invariant on the augmented space  $\mathcal{S}$ , and hence  $\pi$ -invariant on  $\mathcal{X}$ . The result is a straightforward application of Tierney (1998, Theorem 2) on the augmented space  $\mathcal{S}$ . Note that while this work focuses on step size parameters  $\theta \in \mathbb{R}_+$ , Proposition 4.2 below holds for general parameter spaces  $\Theta$  and tuning refreshment distributions  $\eta(d\theta|x, z, a, b)$ .

**Assumption 4.1.** For each  $\theta \in \Theta$ ,  $f_\theta$  is a continuously differentiable involution.

**Proposition 4.2.** Under Assumption 4.1, AutoStep MCMC is  $\bar{\pi}$ -invariant, and hence the  $\mathcal{X}$ -marginal is  $\pi$ -invariant.

### 4.2 Irreducibility and aperiodicity

Next, we establish that the  $\mathcal{X}$ -marginal of AutoStep MCMC is  $\pi$ -irreducible and aperiodic (see Roberts and

Rosenthal (2004)): intuitively, the chain has a positive probability of eventually visiting any measurable  $A \subseteq \mathcal{X}$  with  $\pi(A) > 0$ , and it does not visit various sets in a repeating pattern. We will demonstrate  $\pi$ -irreducibility and aperiodicity simultaneously by showing that the  $\mathcal{X}$ -component of the chain can reach any measurable set  $A \subseteq \mathcal{X}$  in a *single* step with positive probability (*one-step irreducibility*). The first assumption needed is that for any fixed  $\theta \in \Theta$ , the  $\mathcal{X}$ -marginal kernel  $P_\theta(x, \cdot)$  of the original involutive MCMC algorithm given by Eqs. (1) and (2) can do so as well.

**Assumption 4.3.** For all  $x \in \mathcal{X}$ ,  $\theta \in \Theta$ , and  $A \subseteq \mathcal{X}$  such that  $\pi(A) > 0$ , the  $\mathcal{X}$ -marginal kernel  $P_\theta$  of involutive MCMC (Eqs. (1) and (2)) satisfies  $P_\theta(x, A) > 0$ .

The second assumption needed is that there is a non-null set of parameters  $\theta \in \Theta$  that can be selected and result in an accepted move from any point  $x, z \in \mathcal{X} \times \mathcal{Z}$  in the original augmented space of involutive MCMC. We encode this using the positivity of the function

$$\gamma(x, z, \theta) = \int \min\{\eta(\theta | x, z, a, b), \eta(\theta | f_\theta(x, z), a, b)\} \mathbf{1}_\Delta(d(a, b)).$$

**Assumption 4.4.** There exists a  $B \subseteq \Theta$  such that  $\int_B d\theta > 0$  and for all  $x \in \mathcal{X}$ ,  $m$ -a.e.  $z \in \mathcal{Z}$ , and  $\theta \in B$ ,

$$\gamma(x, z, \theta) > 0.$$

These assumptions yield the desired result, which holds for general parameter spaces  $\Theta$  and distributions  $\eta$ .

**Proposition 4.5.** If both Assumptions 4.3 and 4.4 hold, then AutoStep MCMC is one-step irreducible, and hence irreducible and aperiodic.

We now apply Proposition 4.5 to the case where  $\theta$  is a step size parameter and we use  $\eta$  from Section 3.1. In this setting, Assumption 4.4 can be simplified to conditions on the target  $\pi$  and jitter  $\sigma^2$ . Recall that  $\sigma^2 = 0$  formally indicates that  $\eta$  is a Dirac delta.

**Corollary 4.6.** Suppose  $\Theta = (0, \infty)$ , Assumption 4.3 holds, and we use  $\eta$  from Section 3.1. Then, AutoStep MCMC is irreducible and aperiodic if  $\sigma^2 > 0$ , or if for all  $x \in \mathcal{X}$  and  $m$ -a.e.  $z \in \mathcal{Z}$ ,  $|\ell(x, z, \theta_0)| \notin \{0, \infty\}$ .

We show in Lemmas A.1 and A.2 that Assumption 4.3 holds for both RWMH and MALA under weak conditions, and hence the irreducibility and aperiodicity of AutoStep RWMH and MALA follows from either  $\sigma^2 > 0$  or  $|\ell(x, z, \theta_0)| \notin \{0, \infty\}$ .

### 4.3 Step size selector termination

We now establish that under mild conditions, the step size selector function  $\mu$  can be computed in finite-time.

For starting state  $s = (x, z, a, b)$  and initial step size  $\theta_0 > 0$ , let  $\tau(s, \theta_0) \geq 1$  be the number of iterations of the while loop in Algorithm 2.

**Assumption 4.7.**  $\pi(x)$  and  $m(z)$  are continuous, and both  $\lim_{|x| \rightarrow \infty} \pi(x) = 0$  and  $\lim_{|z| \rightarrow \infty} m(z) = 0$ .

**Assumption 4.8.** For any  $(x, z) \in \mathcal{X} \times \mathcal{Z}$ , we have

$$\begin{aligned} \lim_{\theta \rightarrow 0^+} f_\theta(x, z) &= (x, z) & \lim_{\theta \rightarrow 0^+} |\nabla f_\theta(x, z)| &= 1 \\ \lim_{\theta \rightarrow \infty} \|f_\theta(x, z)\| &= +\infty & \limsup_{\theta \rightarrow \infty} |\nabla f_\theta(x, z)| &< +\infty. \end{aligned}$$

**Proposition 4.9.** Let  $\theta_0 > 0$  and suppose Assumptions 4.7 and 4.8 hold. Then  $\tau(s, \theta_0) < \infty$ ,  $\bar{\pi}$ -a.s.

#### 4.4 Energy jump distance

For  $s = (x, z, a, b, \theta) \sim \bar{\pi}$ ,  $s' = \bar{f}(s) = (x', z', a', b', \theta')$ , and  $U \sim \text{Unif}[0, 1]$ , define the *energy jump distance*

$$D = |\ell(x, z, \theta)| \mathbf{1} \left[ U \leq \frac{\bar{\pi}(s')}{\bar{\pi}(s)} J(s) \right],$$

which we use to encode the change in  $\log(\pi(x)m(z))$  after one iteration of AutoStep MCMC. Proposition 4.10 shows that *any* involutive MCMC method—both traditional and AutoStep methods—have an expected energy jump distance bounded above by a simple expression via the tuning parameter proposal density ratio  $\bar{\eta}$ ,

$$\bar{\eta} = \text{ess sup}_{x, z, a, b, \theta} \frac{\eta(\theta | f_\theta(x, z), a, b)}{\eta(\theta | x, z, a, b)} \quad (\text{under } \bar{\pi}).$$

**Proposition 4.10.** Under Assumption 4.1,

$$\mathbb{E}D \leq 2\bar{\eta} \max\{e^{-1}, \bar{\eta} \log \bar{\eta}\}.$$

In particular, for traditional involutive MCMC with a fixed parameter  $\theta = \theta_0$ , or for AutoStep MCMC with  $\sigma^2 = 0$ , or AutoStep MCMC with a fixed-width uniform distribution for  $\eta$ , we have that  $\bar{\eta} \leq 1$ , so

$$\mathbb{E}D \leq 2e^{-1} \approx 0.736.$$

The step size selector presented in Section 3.1 is a computationally efficient method to make  $|\ell(x, z, \theta)|$  fall roughly in the range  $(|\log b|, |\log a|)$ , where  $a, b \sim \text{Unif}(\Delta)$ . Therefore, as a heuristic, we expect

$$0.5 = \mathbb{E}|\log b| \lesssim \mathbb{E}|\ell(x, z, \theta)| \lesssim \mathbb{E}|\log a| = 1.5,$$

with departures from exactness arising due to the discrete doubling/halving procedure (as opposed to an exact root finder). In other words, the step size selector in this work creates proposals with mean energy jump distance roughly targeting the maximum  $\approx 0.736$  for a broad class of involutive MCMC methods.

## 5 EXPERIMENTS

In this section we present an empirical evaluation of three AutoStep MCMC variants: RWMH, MALA, and HMC. We first compare the performance of these methods to their corresponding standard fixed-step-size methods. We then examine the effects of randomization and symmetric thresholds on step size selection, in comparison to previously used deterministic step sizes without symmetric thresholds. Finally, we investigate the effect of tuning the step size selection noise on performance and stability.

Throughout, we measure the efficiency of each sampler in terms of effective sample size (ESS) (Flegal et al., 2008) per unit cost. The ESS we report (minESS) is the minimum of the standard estimate based on autocorrelation (Gelman et al., 2013, p. 286-287) and the estimate with known first and second moments (Galil L Jones and Neath, 2006, p. 1539-1541) across each target dimension, with moments obtained via a separate long run of parallel tempering with Pigeons.jl (Surjanovic et al., 2023). Because we compare gradient and non-gradient methods coded in multiple languages, we use an implementation-independent measure of cost,  $N_\ell + \alpha N_g$ , where  $N_\ell$  is the number of log-target density function calls,  $N_g$  is the number of log-target gradient calls, and  $\alpha$  is the ratio of the average time for a gradient and density call, estimated using 1,000 random samples from each target. See Appendix B for the  $\alpha$  estimates. Unless otherwise specified, all results include 30 independent trials, algorithms are run until the reported minESS exceeds 100, and we use round-based adaptation for all parameters in AutoStep MCMC.

### 5.1 Comparison with existing methods

We first assess the performance of the three variants of AutoStep MCMC with the corresponding standard fixed-step-size methods by comparing their mean energy jump distance ( $D$  from Section 4.4) and minESS per cost on a set of benchmark models. For the fixed step size methods, we considered step sizes  $\{0.1, 0.25, 1.0, 4.0, 10.0\} \times$  the tuned  $\theta_0$  from AutoStep RWMH, and used round-based adaptive tuning for the preconditioner. The benchmarks include two synthetic distributions—Neal’s funnel and the banana distribution—and two real Bayesian posteriors—logistic regression with a horseshoe prior (Carvalho et al., 2009) on the sonar dataset (Sejnowski and Gorman, 1988), and an mRNA transfection model (Ballnus et al., 2017).

Fig. 2 shows the results for RWMH and AutoStep RWMH; see Appendix B for the same set of results for MALA and HMC. This figure demonstrates that the AutoStep method provides a consistently high en-

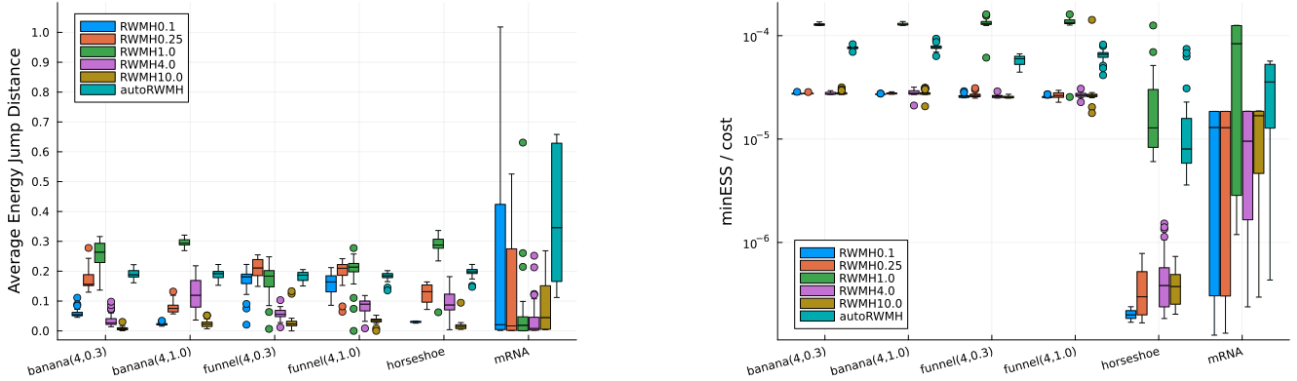


Figure 2: Average energy jump distance (left) and  $\text{minESS}$  per unit cost (right) for AutoStep RWMH and standard RWMH with the fixed step size set to  $\{0.1, 0.25, 1.0, 4.0, 10.0\} \times$  the tuned  $\theta_0$  from AutoStep RWMH.

energy jump distance and  $\text{minESS}$  per unit cost across all benchmarks; it is competitive with the manually tuned method in all cases. Note that AutoStep RWMH requires no manual tuning and thus presents favorable performance with a minimum of user tuning effort.

## 5.2 Effect of jitter and symmetric thresholds

Figure 3 presents the effect of jitter and the use of symmetric step size selector thresholds for AutoStep HMC, MALA and RWMH. Each sampler is tested with four different configurations: the original setting (with asymmetric thresholds used in [Biron-Lattes et al. \(2024\)](#)), with symmetric thresholds, with auto-tuned jitter, and with both symmetric thresholds and auto-tuned jitter. Simulations were conducted on several synthetic targets including the banana distribution, Neal’s funnel distribution, and a multivariate Gaussian distribution (Appendix B), each with different dimensions and scales. The plots demonstrate consistent performance across all sampler variants, with occasional improvements observed when using symmetric thresholds versus asymmetric thresholds (particularly for RWMH). Based on the consistent performance but improved theoretical guarantees, it is generally recommended to use AutoStep MCMC with both symmetric thresholds and auto-tuned jitter.

## 5.3 Stability of round-based jitter tuning

We examine the convergence of the jitter standard deviation  $\sigma$  during round-based tuning. The three plots in Figure 4 show the evolution of the jitter standard deviation across sampling rounds for the three AutoStep MCMC algorithms applied to five different targets. Figure 4 shows that in early tuning rounds the jitter standard deviation varies due to the use of relatively small sample sizes, but eventually stabilizes and converges as the rounds progress. An interesting

observation is that across a wide range of targets, the jitter standard deviation tends to converge to  $\approx 0.1$ ; we leave a deeper investigation of this observation as an open question.

## 5.4 Effect of round-based jitter tuning

Figure 5 shows an investigation of the effect of fixed ( $\sigma = 0, 0.1, 0.5, 2$ ) and tuned jitter standard deviation in AutoStep MCMC. It is evident from Figure 5 that the choice of jitter distribution significantly impacts the efficiency of the sampler. Lower  $\sigma$  (0.1 and 0.5) generally yield higher  $\text{minESS}$  per cost, particularly for more challenging targets. The auto tuned jitter seems to prevent catastrophic failures, while any other fixed value of  $\sigma$  has cases where performance suffers dramatically. Based on these results, the tuned jitter is recommended as a default, as it provides reliable performance without the need for manual tuning.

# 6 CONCLUSION

In this paper we presented AutoStep MCMC, a general locally-adaptive step size selection method for involutive MCMC. We proved that AutoStep MCMC kernels are  $\pi$ -invariant, irreducible, and aperiodic under mild conditions. We also provided upper bounds on the mean energy jump distance for a general class of involutive MCMC methods. We demonstrated empirically that AutoStep MCMC is competitive with well-tuned standard involutive methods, and that the proposed methods are stable and reliable. One promising direction for future work is a rigorous theoretical analysis of the sampling efficiency of AutoStep MCMC in terms of expected squared jump distance, asymptotic variance, and total variation distance.

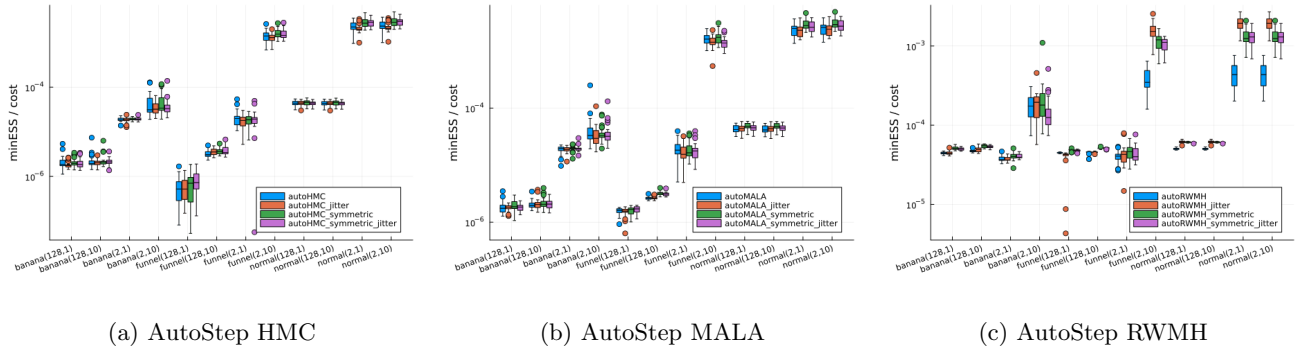


Figure 3: Comparison of different versions of AutoStep MCMC on the funnel, banana, and Gaussian distributions with varying dimensions and scales, denoted “model(dimension, scale)”. We use “jitter” to indicate that the sampler uses an auto-tuned jitter, and “symmetric” to denote that the sampler uses symmetric thresholds.

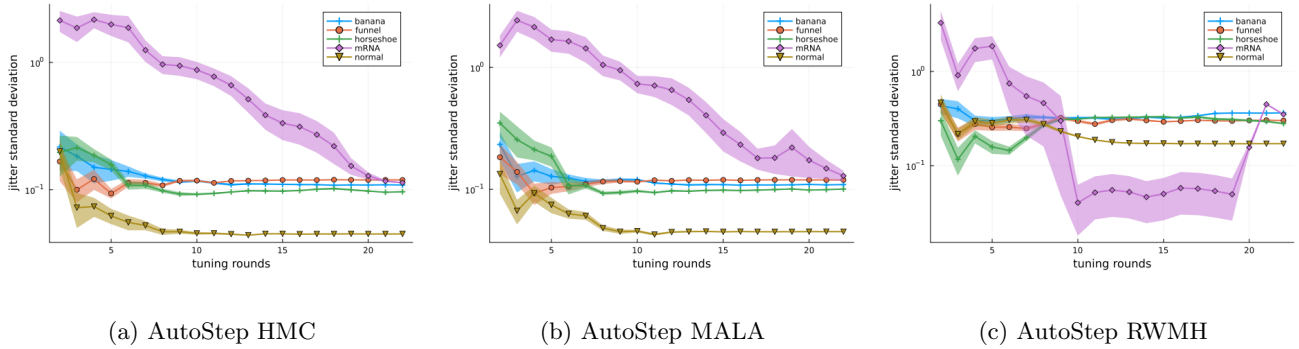


Figure 4: Convergence of the jitter standard deviation  $\sigma$  across sampling rounds for AutoStep MCMC.

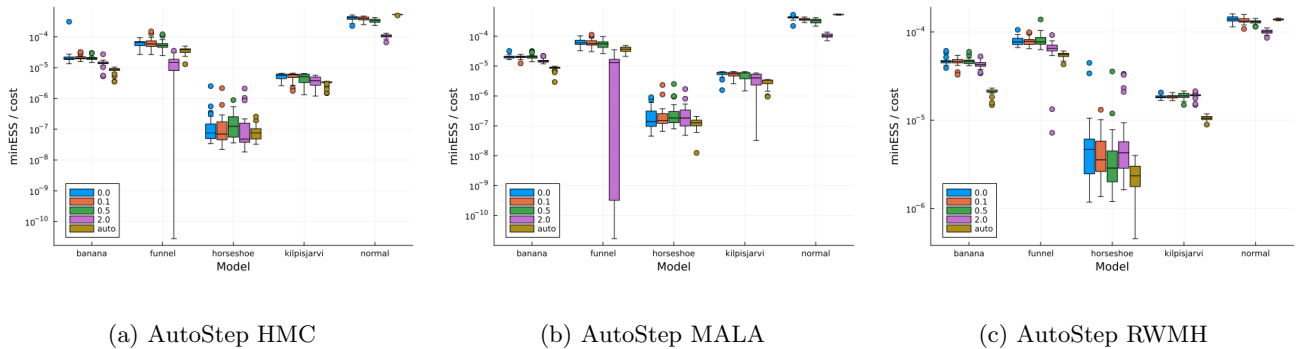


Figure 5: Comparison of tuned and fixed jitter. For the banana and funnel distributions, we set  $\text{dim} = 2$  and  $\text{scale} = 1$ .



---

## Acknowledgements

ABC and TC acknowledge the support of an NSERC Discovery Grant. TL acknowledges the support of the UBC Advanced Machine Learning Training Network. NS acknowledges the support of a Vanier Canada Graduate Scholarship. We additionally acknowledge use of the ARC Sockeye computing platform from the University of British Columbia.

## References

- Andrieu, C., Lee, A., and Livingstone, S. (2020). A general perspective on the Metropolis–Hastings kernel. *arXiv:2012.14881*.
- Andrieu, C. and Thoms, J. (2008). A tutorial on adaptive MCMC. *Statistics and Computing*, 18(4):343–373.
- Atchadé, Y. F. (2006). An adaptive version for the Metropolis adjusted Langevin algorithm with a truncated drift. *Methodology and Computing in Applied Probability*, 8(2):235–254.
- Ballnus, B., Hug, S., Hatz, K., Görlitz, L., Hasenauer, J., and Theis, F. J. (2017). Comprehensive benchmarking of Markov chain Monte Carlo methods for dynamical systems. *BMC Systems Biology*.
- Bélisle, C., Romeijn, E., and Smith, R. (1993). Hit-and-run algorithms for generating multivariate distributions. *Mathematics of Operations Research*, 18(2):255–266.
- Biron-Lattes, M., Surjanovic, N., Syed, S., Campbell, T., and Bouchard-Côté, A. (2024). autoMALA: Locally adaptive Metropolis-adjusted Langevin algorithm. In *International Conference on Artificial Intelligence and Statistics*, volume 238, pages 4600–4608.
- Bou-Rabee, N., Carpenter, B., Kleppe, T. S., and Marsden, M. (2024a). Incorporating local step-size adaptivity into the No-U-Turn Sampler using Gibbs self tuning. *arXiv: 2408.08259*.
- Bou-Rabee, N., Carpenter, B., and Marsden, M. (2024b). GIST: Gibbs self-tuning for locally adaptive Hamiltonian Monte Carlo. *arXiv:2404.15253*.
- Carvalho, C. M., Polson, N. G., and Scott, J. G. (2009). Handling sparsity via the horseshoe. In *International Conference on Artificial Intelligence and Statistics*, volume 5, pages 73–80.
- Chimisov, C., Latuszynski, K., and Roberts, G. (2018). Air Markov chain Monte Carlo. *arXiv:1801.09309*.
- Coullon, J., South, L., and Nemeth, C. (2023). Efficient and generalizable tuning strategies for stochastic gradient MCMC. *Statistics and Computing*, 33(3):66.
- Duane, S., Kennedy, A., Pendleton, B. J., and Roweth, D. (1987). Hybrid Monte Carlo. *Physics Letters B*, 195(2):216–222.
- Flegal, J. M., Haran, M., and Jones, G. L. (2008). Markov chain Monte Carlo: Can we trust the third significant figure? *Statistical Science*, 23(2).
- Galin L Jones, Murali Haran, B. S. C. and Neath, R. (2006). Fixed-width output analysis for Markov chain Monte Carlo. *Journal of the American Statistical Association*, 101(476):1537–1547.
- Ge, H., Xu, K., and Ghahramani, Z. (2018). Turing: A language for flexible probabilistic inference. In *International Conference on Artificial Intelligence and Statistics*, pages 1682–1690.
- Gelman, A., Carlin, J., Stern, H., Dunson, D., Vehtari, A., and Rubin, D. (2013). *Bayesian Data Analysis*. CRC Press, 3rd edition.
- Girolami, M. and Calderhead, B. (2011). Riemann manifold Langevin and Hamiltonian Monte Carlo methods. *Journal of the Royal Statistical Society: Series B (Statistical Methodology)*, 73(2):123–214.
- Green, P. and Mira, A. (2001). Delayed rejection in reversible jump Metropolis–Hastings. *Biometrika*, 88(4):1035–1053.
- Haario, H., Saksman, E., and Tamminen, J. (2001). An adaptive Metropolis algorithm. *Bernoulli*, 7(2):223–242.
- Hastings, W. K. (1970). Monte Carlo sampling methods using Markov chains and their applications. *Biometrika*, 57(1):97–109.
- Hoffman, M. D. and Gelman, A. (2014). The No-U-Turn Sampler: Adaptively setting path lengths in Hamiltonian Monte Carlo. *The Journal of Machine Learning Research*, 15(1):1593–1623.
- Kleppe, T. S. (2016). Adaptive step size selection for Hessian-based manifold Langevin samplers. *Scandinavian Journal of Statistics*, 43(3):788–805.
- Livingstone, S. (2021). Geometric ergodicity of the random walk Metropolis with position-dependent proposal covariance. *Mathematics*, 9(4).
- Maire, F. and Vandekerckhove, P. (2022). Markov kernels local aggregation for noise vanishing distribution sampling. *SIAM Journal on Mathematics of Data Science*, 4(4):1293–1319.
- Marshall, T. and Roberts, G. (2012). An adaptive approach to Langevin MCMC. *Statistics and Computing*, 22.
- Metropolis, N., Rosenbluth, A. W., Rosenbluth, M. N., Teller, A. H., and Teller, E. (1953). Equation of state calculations by fast computing machines. *The Journal of Chemical Physics*, 21(6):1087–1092.

- Modi, C., Barnett, A., and Carpenter, B. (2023). Delayed rejection Hamiltonian Monte Carlo for sampling multiscale distributions. *Bayesian Analysis*, pages 1–28.
- Neal, R. M. (1996). *Bayesian Learning for Neural Networks*, volume 118 of *Lecture Notes in Statistics*. Springer New York, New York, NY, 1 edition.
- Neal, R. M. (2003). Slice sampling. *The Annals of Statistics*, 31(3):705–767.
- Neklyudov, K., Shvechikov, P., and Vetrov, D. (2018). Metropolis-Hastings view on variational inference and adversarial training. *arXiv:1810.07151*.
- Neklyudov, K., Welling, M., Egorov, E., and Vetrov, D. (2020). Involutive MCMC: A unifying framework. In *International Conference on Machine Learning*.
- Nishimura, A. and Dunson, D. (2016). Variable length trajectory compressible hybrid Monte Carlo. *arXiv:1604.00889*.
- Polson, N. G. and Scott, J. G. (2012). On the half-Cauchy prior for a global scale parameter. *Bayesian Analysis*, 7(4):887–902.
- Roberts, G., Gelman, A., and Gilks, W. (1997). Weak convergence and optimal scaling of random walk Metropolis algorithms. *Annals of Applied Probability*, 7(1):110–120.
- Roberts, G. and Rosenthal, J. (2004). General state space Markov chains and MCMC algorithms. *Probability Surveys*, 1:20–71.
- Roberts, G. O. and Rosenthal, J. S. (1998). Optimal scaling of discrete approximations to Langevin diffusions. *Journal of the Royal Statistical Society. Series B (Statistical Methodology)*, 60(1):255–268.
- Rosky, P. J., Doll, J. D., and Friedman, H. L. (1978). Brownian dynamics as smart Monte Carlo simulation. *The Journal of Chemical Physics*, 69(10):4628–4633.
- Sejnowski, T. and Gorman, R. (1988). Connectionist Bench (Sonar, Mines vs. Rocks). UCI Machine Learning Repository.
- Surjanovic, N., Biron-Lattes, M., Tiede, P., Syed, S., Campbell, T., and Bouchard-Côté, A. (2023). Pigeons.jl: Distributed sampling from intractable distributions. *arXiv:2308.09769*.
- Tierney, L. (1998). A note on Metropolis–Hastings kernels for general state spaces. *The Annals of Statistics*, 8(1):1–9.
- Tierney, L. and Mira, A. (1999). Some adaptive Monte Carlo methods for Bayesian inference. *Statistics in Medicine*, 18:2507–2515.
- Turok, G., Modi, C., and Carpenter, B. (2024). Sampling from multiscale densities with delayed rejection generalized Hamiltonian Monte Carlo. *arXiv:2406.02741*.

---



---

## Supplementary Materials

---

### A Proofs

*Proof of Proposition 4.2.* The auxiliary refreshment and tuning parameter refreshment steps in AutoStep MCMC (Steps 1. and 2.) resample  $(z, a, b, \theta)$  jointly from their conditional distribution given  $x$  under  $\bar{\pi}$ . This move is well-known to be  $\bar{\pi}$ -invariant, and so it remains only to show that the Metropolis-corrected involutive proposal (Steps 3. and 4.) is  $\bar{\pi}$ -invariant. The kernel for the proposal on the augmented space  $\mathcal{S}$  is

$$Q(s, ds') = \delta_{\bar{f}(s)}(ds'),$$

and the acceptance probability  $\alpha : \mathcal{S}^2 \rightarrow \mathbb{R}_+$  is given by

$$\alpha(s, s') = \min \left\{ 1, \frac{\bar{\pi}(s')}{\bar{\pi}(s)} J(s) \right\}.$$

In the notation of Tierney (1998, Theorem 2), define the measure  $\mu(ds, ds') = \bar{\pi}(ds)\delta_{\bar{f}(s)}(ds')$ ; because  $\bar{f}$  is an involution, we have that the symmetric set  $R$  and density ratio  $r : R \rightarrow \mathbb{R}_+$  are given by

$$R = \{(s, s') \in \mathcal{S}^2 : \bar{f}(s) = s', \bar{\pi}(s) > 0, \bar{\pi}(s') > 0\}, \quad r(s, s') = \frac{\bar{\pi}(ds)\delta_{\bar{f}(s)}(ds')}{\bar{\pi}(ds')\delta_{\bar{f}(s')}(ds)}.$$

Note that condition (i) of Tierney (1998, Theorem 2) holds by definition of  $R$  and  $\alpha$ . Suppose for the moment that  $r(s, s') = \frac{\bar{\pi}(s)}{\bar{\pi}(s')} J(s')$ ; then condition (ii)—and hence  $\bar{\pi}$ -invariance—holds because

$$\alpha(s, s')r(s, s') = \min \left\{ 1, \frac{\bar{\pi}(s')}{\bar{\pi}(s)} J(s) \right\} \frac{\bar{\pi}(s)}{\bar{\pi}(s')} J(s') = \min \left\{ \frac{\bar{\pi}(s)}{\bar{\pi}(s')} J(s'), J(s')J(s) \right\} = \alpha(s', s),$$

which follows because  $J(s)J(s') = 1$   $\mu$ -a.e. on  $R$ . To demonstrate that  $r(s, s')$  has the required form, consider a test function  $g : \mathcal{S}^2 \rightarrow \mathbb{R}$ :

$$\begin{aligned} \int g(s, s') \bar{\pi}(ds) \delta_{\bar{f}(s)}(ds') &= \int g(s, \bar{f}(s)) \bar{\pi}(ds) \\ &= \int g((x, z, a, b, \theta), (f_\theta(x, z), a, b, \theta)) \bar{\pi}(x, z, a, b, \theta) dx dz d(a, b) d\theta. \end{aligned}$$

Since  $f_\theta$  is a continuously differentiable involution, we can transform variables  $x', z' = f_\theta(x, z)$  by including a Jacobian term  $J(s) = |\nabla f_\theta(x, z)|$  in the integrand and by noting  $x, z = f_\theta(x', z')$ :

$$\begin{aligned} &= \int g((f_\theta(x', z'), a, b, \theta), (x', z', a, b, \theta)) \bar{\pi}(f_\theta(x', z'), a, b, \theta) |\nabla f_\theta(x', z')| dx' dz' d(a, b) d\theta \\ &= \int g(\bar{f}(s'), s') \bar{\pi}(\bar{f}(s')) J(s') ds' \\ &= \int g(\bar{f}(s'), s') \frac{\bar{\pi}(\bar{f}(s'))}{\bar{\pi}(s')} J(s') \bar{\pi}(ds') \\ &= \int g(s, s') \frac{\bar{\pi}(s)}{\bar{\pi}(s')} J(s') \bar{\pi}(ds') \delta_{\bar{f}(s')}(ds). \end{aligned}$$

Examining the first and last integral expressions, the density ratio has the form

$$r(s, s') = \frac{\bar{\pi}(ds)\delta_{\bar{f}(s)}(ds')}{\bar{\pi}(ds')\delta_{\bar{f}(s')}(ds)} = \frac{\bar{\pi}(s)}{\bar{\pi}(s')} J(s').$$

□

*Proof of Proposition 4.5.* Let  $K(x, \cdot)$  denote the Markov kernel for the  $\mathcal{X}$ -marginal process of AutoStep MCMC. Since for  $u, v \geq 0$ ,  $\min\{1, uv\} \geq \min\{1, u\} \min\{1, v\}$ , we have that for  $s = (x, z, a, b, \theta)$ ,

$$\min\left\{1, \frac{\bar{\pi}(\bar{f}(s))}{\bar{\pi}(s)} J(s)\right\} \geq \min\left\{1, e^{\ell(x, z, \theta)}\right\} \min\left\{1, \frac{\eta(\theta | f_\theta(x, z), a, b)}{\eta(\theta | x, z, a, b)}\right\}.$$

Therefore

$$\begin{aligned} K(x, A) &\geq \int \mathbf{1}[f_\theta(x, z) \in A \times \mathcal{Z}] \min\left\{1, e^{\ell(x, z, \theta)}\right\} \min\left\{1, \frac{\eta(\theta | f_\theta(x, z), a, b)}{\eta(\theta | x, z, a, b)}\right\} \eta(d\theta | x, z, a, b) m(dz) \mathbf{1}_\Delta(d(a, b)) \\ &= \int \mathbf{1}[f_\theta(x, z) \in A \times \mathcal{Z}] \min\left\{1, e^{\ell(x, z, \theta)}\right\} \gamma(x, z, \theta) m(dz) d\theta, \end{aligned}$$

where

$$\gamma(x, z, \theta) = \int \min\{\eta(\theta | x, z, a, b), \eta(\theta | f_\theta(x, z), a, b)\} \mathbf{1}_\Delta(d(a, b)).$$

By Assumption 4.4, for all  $x \in \mathcal{X}$ ,  $m$ -a.e.  $z \in \mathcal{Z}$ , and for all  $\theta \in B$  where  $\int_B d\theta > 0$ ,  $\gamma(x, z, \theta) > 0$ . Therefore

$$\begin{aligned} &\int \mathbf{1}[f_\theta(x, z) \in A \times \mathcal{Z}] \min\left\{1, e^{\ell(x, z, \theta)}\right\} \gamma(x, z, \theta) m(dz) \mathbf{1}[\theta \in B] d\theta > 0 \\ \iff &\int \mathbf{1}[f_\theta(x, z) \in A \times \mathcal{Z}] \min\left\{1, e^{\ell(x, z, \theta)}\right\} m(dz) \mathbf{1}[\theta \in B] d\theta > 0. \end{aligned}$$

The proof concludes by noting that

$$\int \mathbf{1}[f_\theta(x, z) \in A \times \mathcal{Z}] \min\left\{1, e^{\ell(x, z, \theta)}\right\} m(dz) \mathbf{1}[\theta \in B] d\theta = \int P_\theta(x, A) \mathbf{1}[\theta \in B] d\theta,$$

where  $P_\theta(x, A)$  is the one-step probability of transitioning into  $A$  from  $x$  for the original involutive chain with parameter  $\theta$ , and then by applying Assumption 4.3.  $\square$

*Proof of Corollary 4.6.* The proof involves verifying Assumption 4.4. When  $\sigma^2 > 0$ , for all  $x \in \mathcal{X}$ ,  $z \in \mathcal{Z}$ ,  $\eta$  is a normal distribution and has full support, and so  $\gamma(x, z, \theta) > 0$ . For the latter case, without loss of generality we can assume  $\sigma^2 = 0$  (since if  $\sigma^2 > 0$ , the previous case applies). Therefore,  $d\theta$  is concentrated on  $\{\theta = \theta_0 \times 2^j : j \in \mathbb{Z}\}$ . Consider setting  $B = \{\theta_0\}$ . Assumption 4.4 holds if for all  $x \in \mathcal{X}$  and  $m$ -a.e.  $z \in \mathcal{Z}$ ,

$$\int \mathbf{1}[\mu(x, z, a, b) = \theta_0 = \mu(f_{\theta_0}(x, z), a, b)] \mathbf{1}_\Delta(d(a, b)) > 0.$$

That is, if there is a nonzero probability of choosing the default parameter  $\theta_0$  at any point  $(x, z)$ . Note that

$$\begin{aligned} \mu(x, z, a, b) = \theta_0 &= \mu(f_{\theta_0}(x, z), a, b) \\ \iff \log(a) < \ell(x, z, \theta_0) < \log(b) &\quad \text{or} \quad \log(a) < -\ell(x, z, \theta_0) < \log(b). \end{aligned}$$

By assumption, for all  $x \in \mathcal{X}$  and  $m$ -a.e.  $z \in \mathcal{Z}$ , we have  $\ell(x, z, \theta_0) \notin \{-\infty, 0, \infty\}$ . If  $\ell(x, z, \theta_0) > 0$ , then when  $a < \exp(-\ell(x, z, \theta_0)) < b$  we have the condition hold. This has positive measure under  $\mathbf{1}_\Delta(d(a, b))$ . If  $\ell(x, z, \theta_0) < 0$ , then when  $a < \exp(\ell(x, z, \theta_0)) < b$ , the above condition holds. This set also has positive measure.  $\square$

**Lemma A.1.** *For the AutoStep RWMH kernel with any fixed  $\theta > 0$ ,  $x \in \mathcal{X}$ , and  $A \subset \mathcal{X}$  with  $\pi(A) > 0$ , we have  $P_\theta(x, A) > 0$ , provided that  $\pi(x) > 0$  for all  $x \in \mathcal{X}$ .*

*Proof of Lemma A.1.* Fix  $\theta > 0$ ,  $A \subset \mathcal{X}$  with  $\pi(A) > 0$  and  $x \in \mathcal{X}$ . Because  $\pi \ll \lambda$ , we have  $\lambda(A) > 0$ . By translation properties of the Lebesgue measure, for any  $x \in \mathbb{R}^d$ ,  $\lambda(A) = \lambda(A - x) > 0$ , where  $A - x = \{\tilde{x} - x : \tilde{x} \in A\}$ . Here,  $(x', z') = f_\theta(x, z) = (x + z, -z)$  and so  $|\nabla f_\theta(x, z)| = 1$ . Also, since  $z \sim m$  where  $m = \mathcal{N}(0, I)$ , we have

$$\ell(x, z, \theta) = \log\left(\frac{\pi(x')}{\pi(x)}\right).$$

Then,

$$P_\theta(x, A) \geq \int \mathbf{1}[z \in A - x] \min\left\{1, \frac{\pi(x+z)}{\pi(x)}\right\} m(z) \lambda(dz) > 0,$$

because for all  $x, z$  we have  $\lambda(A - x) > 0$ ,  $m(z) > 0$ , and  $\min\{1, \pi(x+z)/\pi(x)\} > 0$ .  $\square$

**Lemma A.2.** *For the AutoStep MALA kernel with any fixed  $\theta > 0$ ,  $x \in \mathcal{X}$ , differentiable  $\pi$ , positive definite  $M$ , and  $A \subset \mathcal{X}$  with  $\pi(A) > 0$ , we have  $P_\theta(x, A) > 0$ , provided that  $\pi(x) > 0$  for all  $x \in \mathcal{X}$ .*

*Proof of Lemma A.2.* Fix  $\theta > 0$ ,  $A \subset \mathcal{X}$  with  $\pi(A) > 0$  and  $x \in \mathcal{X}$ . Because  $\pi \ll \lambda$ , we have  $\lambda(A) > 0$ . As in [Biron-Lattes et al. \(2024\)](#), we combine the updates on  $(x, z)$  into one step, so that  $f_\theta(x, z) = (x'(\theta), z'(\theta))$ , where

$$x'(\theta) = x + \theta M^{-1} z + \frac{\theta^2}{2} M^{-1} \nabla \log \gamma(x), \quad z'(\theta) = - \left( z + \frac{\theta}{2} \nabla \log \gamma(x) + \frac{\theta}{2} \nabla \log \gamma(x'(\theta)) \right).$$

Now,  $x'(\theta) \in A$  if

$$z \in A_x := \left\{ \frac{M(\tilde{x} - x)}{\theta} - \frac{\theta}{2} \nabla \log \gamma(x) : \tilde{x} \in A \right\}.$$

By translation and scaling properties of the Lebesgue measure, for any  $x \in \mathbb{R}^d$ ,  $\lambda(A_x) > 0$ . It is a standard result that the leapfrog integrator satisfies  $|\nabla f_\theta(x, z)| = 1$ . We have

$$\ell(x, z, \theta) = \log \left( \frac{\pi(x') m(z')}{\pi(x) m(z)} \right).$$

Then,

$$P_\theta(x, A) \geq \int \mathbf{1}[z \in A_x] \min\left\{1, \frac{\pi(x') m(z')}{\pi(x) m(z)}\right\} m(z) \lambda(dz) > 0.$$

because for all  $x, z$  we have  $\lambda(A_x) > 0$ ,  $m(z) > 0$ , and the acceptance ratio is positive.  $\square$

*Proof of Proposition 4.9.* We generalize the step size termination proof of Theorem 3.3 by [Biron-Lattes et al. \(2024\)](#). We consider two cases:  $v = 1$  on Line 3 of Algorithm 2, and  $v = -1$ . Fix any  $(x, z) \in \mathcal{X} \times \mathcal{Z}$  and  $\theta_0 > 0$ . We assume that  $\pi(x) > 0$  and  $m(z) > 0$ , which holds  $\bar{\pi}$ -almost surely.

If  $v = -1$ , we have  $|\ell_0| > |\log(a)|$ , which implies either  $\ell_0 < \log(a)$  or  $-\ell_0 < \log(a)$ . This means that the initial step size  $\theta_0$  is too large in either the forward or the reverse direction. In this scenario, we start the halving procedure. Now,

$$\ell(x, z, \theta) = \log \left( \frac{\pi(x'(\theta)) m(z'(\theta))}{\pi(x) m(z)} |\nabla f_\theta(x, z)| \right),$$

where  $(x'(\theta), z'(\theta)) = f_\theta(x, z)$ . The step size selection procedure terminates as soon as  $|\ell(\theta)| \leq |\log(a)|$  for some  $\theta = \theta_0 \times 2^j$ ,  $j \in \mathbb{Z}^-$ . By Assumptions 4.7 and 4.8,  $\lim_{\theta \rightarrow 0^+} \ell(x, z, \theta) = 0$ , and so there is a  $0 < \theta' < \theta_0$  with the property that  $|\ell(\theta)| \leq |\log(a)|$  for all  $0 < \theta \leq \theta'$ . Provided that  $|\log(a)| > 0$ , we have  $\tau(s, \theta_0) < \infty$  in this case.

In the case where  $v = 1$ , we have  $|\ell_0| < |\log(b)|$ , which implies  $\ell_0 > \log(b)$  and  $-\ell_0 > \log(b)$ . This means that the initial step size  $\theta_0$  is too small in both the forward and the reverse direction. Here, we start the doubling procedure. The step size selection procedure terminates as soon as  $|\ell(\theta)| \geq |\log(b)|$  for some  $\theta = \theta_0 \times 2^j$ ,  $j \in \mathbb{Z}^-$ . By Assumptions 4.7 and 4.8,  $\lim_{\theta \rightarrow \infty} \ell(x, z, \theta) = -\infty$ . Therefore, there is a  $\theta' > \theta_0$  with the property that  $|\ell(\theta)| \geq |\log(b)|$  for all  $\theta \geq \theta'$ . Provided that  $|\log(b)| < \infty$ , we have  $\tau(s, \theta_0) < \infty$  in this case, as well.  $\square$

*Proof of Proposition 4.10.* The expected jump distance is

$$\mathbb{E}D = \int |\ell(x, z, \theta)| \min\left\{1, e^{\ell(x, z, \theta)} \frac{\eta(\theta | f_\theta(x, z), a, b)}{\eta(\theta | x, z, a, b)}\right\} \pi(dx) m(dz) (2\mathbf{1}_\Delta(d(a, b))) \eta(d\theta | x, z, a, b).$$

Let  $A_{\leq} = \{x, z, a, b, \theta : \exp(\ell(x, z, \theta)) \leq \eta(\theta|x, z, a, b)/\eta(\theta|f_{\theta}(x, z), a, b)\}$ , and define  $A_{<}, A_{\geq}, A_{>}$  similarly by replacing the inequality in the definition. We begin by splitting the integral into regions  $A_{\leq}, A_{>}$ :

$$\begin{aligned} \mathbb{E}D &= \int_{A_{>}} |\ell(x, z, \theta)| \pi(\mathrm{d}x) m(\mathrm{d}z) (2\mathbb{1}_{\Delta}(\mathrm{d}(a, b))) \eta(\mathrm{d}\theta | x, z, a, b) \\ &\quad + \int_{A_{\leq}} |\ell(x, z, \theta)| e^{\ell(x, z, \theta)} \eta(\theta|f_{\theta}(x, z), a, b) \pi(\mathrm{d}x) m(\mathrm{d}z) (2\mathbb{1}_{\Delta}(\mathrm{d}(a, b))) \mathrm{d}\theta. \end{aligned}$$

Next we perform the transformation of variables  $x', z' = f_{\theta}(x, z)$  on the  $A_{>}$  integral. Recall that  $\ell(x, z, \theta)$  satisfies

$$\ell(f_{\theta}(x, z), \theta) = -\ell(x, z, \theta),$$

and note that this transformation yields the integration region  $A_{<}$ , such that

$$\begin{aligned} \mathbb{E}D &= \int_{A_{<}} |\ell(x, z, \theta)| e^{\ell(x, z, \theta)} \eta(\theta|f_{\theta}(x, z), a, b) \pi(\mathrm{d}x) m(\mathrm{d}z) (2\mathbb{1}_{\Delta}(\mathrm{d}(a, b))) \mathrm{d}\theta \\ &\quad + \int_{A_{\leq}} |\ell(x, z, \theta)| e^{\ell(x, z, \theta)} \eta(\theta|f_{\theta}(x, z), a, b) \pi(\mathrm{d}x) m(\mathrm{d}z) (2\mathbb{1}_{\Delta}(\mathrm{d}(a, b))) \mathrm{d}\theta. \end{aligned}$$

The upper bound follows by combining the two terms and bounding the  $\eta$  ratio:

$$\begin{aligned} \mathbb{E}D &\leq 2 \int_{A_{\leq}} |\ell(x, z, \theta)| e^{\ell(x, z, \theta)} \frac{\eta(\theta|f_{\theta}(x, z), a, b)}{\eta(\theta|x, z, a, b)} \eta(\mathrm{d}\theta|x, z, a, b) \pi(\mathrm{d}x) m(\mathrm{d}z) (2\mathbb{1}_{\Delta}(\mathrm{d}(a, b))) \\ &\leq 2\bar{\eta} \sup_{y \leq \log \bar{\eta}} |y| e^y \bar{\pi}(A_{\leq}) \\ &\leq 2\bar{\eta} \sup_{y \leq \log \bar{\eta}} |y| e^y \\ &= 2\bar{\eta} \max\{e^{-1}, \bar{\eta} \log \bar{\eta}\}. \end{aligned}$$

□

---

## B Additional Experiments

### B.1 Synthetic and real data models

We present the synthetic and real data models used in Section 5. In the following,  $\mathcal{N}(\mu, \sigma^2)$  represents a normal distribution with mean  $\mu$  and variance  $\sigma^2$ . We write  $\mathcal{T}_n(\mu, \tau)$  to represent the  $t$ -distribution with  $n$  degrees of freedom and specified location and scale, such that if  $x \sim \mathcal{T}_n(\mu, \tau)$  then  $(x - \mu)/\tau$  follows a Student's  $t$ -distribution with  $n$  degrees of freedom. We use  $\mathcal{T}_n(\mu, \tau; b_L, b_U)$  to represent the truncated  $t$ -distribution with location and scale with a lower bound  $b_L$  and an upper bound  $b_U$ . Similarly, we use  $\mathcal{N}(\mu, \sigma^2; b_L, b_U)$  to denote a truncated normal distribution with bounds  $(b_L, b_U)$ .

- The Neal's funnel with  $d$  dimensions ( $d \geq 2$ ) and scale parameter  $\tau > 0$ , denoted by  $\text{funnel}(d, \tau)$ , is given by

$$X_1 \sim \mathcal{N}(0, 9), \quad X_2, \dots, X_d \mid X_1 = x_1 \stackrel{\text{iid}}{\sim} \mathcal{N}(0, \exp(x_1/\tau)).$$

- The banana distribution with  $d$  dimensions and scale parameter  $\tau > 0$ , denoted by  $\text{banana}(d, \tau)$ , is given by

$$X_1 \sim \mathcal{N}(0, 10), \quad X_2, \dots, X_d \mid X_1 = x_1 \stackrel{\text{iid}}{\sim} \mathcal{N}(x_1^2, \tau^2/10).$$

- The  $d$ -dimensional normal distribution with precision parameter  $\tau > 0$ , denoted by  $\text{normal}(d, \tau)$ , is given by

$$X_1, \dots, X_d \stackrel{\text{iid}}{\sim} \mathcal{N}(0, 1/\tau).$$

- The horseshoe model on the sonar dataset with a binary response vector  $y \in \{0, 1\}^n$  and matrix of predictors  $x \in \mathbb{R}^{n \times d}$  is given by

$$\begin{aligned} \tau &\sim \text{Cauchy}(0, 1) \\ \lambda_j &\sim \text{Cauchy}(0, 1), \quad j = 1, \dots, d \\ \beta_0 &\sim \mathcal{T}_3(0, 1) \\ \beta &\sim \mathcal{N}(0, \tau^2 \Lambda), \quad \Lambda = \text{diag}(\lambda_1^2, \dots, \lambda_d^2) \\ y_i \mid \beta_0, \beta, x_i &\sim \text{Bernoulli} \left( \frac{1}{1 + \exp(-(\beta_0 + \sum_{j=1}^d x_{i,j} \beta_j))} \right), \quad i = 1, \dots, n. \end{aligned}$$

- The mRNA model with  $N$  observations, the time  $t \in \mathbb{R}^N$ , and the observed outcomes  $y \in \mathbb{R}^N$  is given by

$$\begin{aligned} \log_{10}(t_0) &\sim \text{Uniform}(-2, 1) \\ \log_{10}(k_0) &\sim \text{Uniform}(-5, 5) \\ \log_{10}(\beta) &\sim \text{Uniform}(-5, 5) \\ \log_{10}(\delta) &\sim \text{Uniform}(-5, 5) \\ \log_{10}(\sigma) &\sim \text{Uniform}(-2, 2) \\ \mu_i &= \begin{cases} 0, & t_i - t_0 \leq 0 \\ k_0 \cdot \frac{\exp(-\beta \cdot (t_i - t_0)) - \exp(-\delta \cdot (t_i - t_0))}{\delta - \beta}, & \text{if } \delta \neq \beta \\ k_0 \cdot (t_i - t_0), & \text{if } \delta = \beta \end{cases}, \quad i = 1, \dots, N \\ y_i \mid \mu_i, \sigma &\sim \mathcal{N}(\mu_i, \sigma^2), \quad i = 1, \dots, N. \end{aligned}$$

- The kilpisjarvi model with the predictors  $x \in \mathbb{R}^N$ , the observed responses  $y \in \mathbb{R}^N$ , and additional parameters  $\mu_\alpha, \mu_\beta, \sigma_\alpha, \sigma_\beta$ , is given by

$$\begin{aligned} \alpha &\sim \mathcal{N}(\mu_\alpha, \sigma_\alpha^2) \\ \beta &\sim \mathcal{N}(\mu_\beta, \sigma_\beta^2) \\ \sigma &\sim \mathcal{N}(0, 1; 0, \infty) \\ y_i \mid \alpha, \beta, \sigma, x_i &\sim \mathcal{N}(\alpha + \beta x_i, \sigma^2), \quad i = 1, \dots, N. \end{aligned}$$

Model	Dimension	$\alpha$	Model	Dimension	$\alpha$
horseshoe	127	35.67	banana(2,10)	2	3.431
mRNA	5	5.767	banana(4,0.3)	4	4.569
kilpisjarvi	3	5.9561	banana(4,1)	4	4.591
funnel(2,1)	2	4.047	banana(128,1)	128	58.94
funnel(2,10)	2	3.572	banana(128,10)	128	57.06
funnel(4,0.3)	4	4.712	normal(2,1)	2	5.674
funnel(4,1)	4	3.847	normal(2,10)	2	5.301
funnel(128,1)	128	65.44	normal(20,1)	20	14.19
funnel(128,10)	128	62.34	normal(128,1)	128	54.15
banana(2,1)	2	3.652	normal(128,10)	128	54.63

 Table 1: The scaling constant  $\alpha$  for each model, as mentioned in Section 5.

## B.2 Estimation of scaling factors

As mentioned in Section 5, we use  $\alpha$  as a target-dependent scaling factor to balance the cost of gradient and density evaluations. To determine  $\alpha$ , we ran three separate Markov chains using Pigeons to obtain draws, benchmarked the time required for gradient computations, and benchmarked the time for log density evaluations. The scaling factor  $\alpha$  is then obtained as the ratio of the total time spent on gradient evaluations to the total time spent on log density evaluations. The chains are long enough such that the estimate error (in absolute difference) is within 2%. The  $\alpha$  values used in all experiments are presented in Table 1.

There seems to be a positive correlation between  $\alpha$  and the dimension of the problems. This correlation is likely due to the auto-differentiation system used to compute gradients. While auto-differentiation avoids the need for manual differentiation, it appears to incur a computational cost that increases with dimensionality.

## B.3 Number of leapfrog steps in AutoStep HMC

Given a number  $L_{\max} \in \mathbb{N}$ , the number of leapfrog steps taken is sampled at each iteration via  $L \sim \text{Unif}\{1 : L_{\max}\}$ , independent of other variables. The algorithm is initialized with  $L_{\max} = 1$ , which means that it exactly matches AutoStep MALA at this stage. Then, at each round we compute the sample autocorrelation  $\rho$  of  $V(x) := \log \pi(x)$ . If  $\rho > 0.99$ , we double the value of  $L_{\max}$ . On the other hand, if  $\rho < 0.95$ , we set  $L_{\max} \leftarrow \max\{1, L_{\max}/2\}$ . Otherwise, we leave this parameter unchanged for the next round.

## B.4 Comparison of AutoStep and fixed-step-size HMC and MALA

To complement the RWMH results shown in Section 5.1, we present the same results for MALA and HMC in Fig. 6. The performance of the AutoStep methods is again consistent across all models in terms of high energy jump distances. In terms of minESS per unit cost, the fixed-step-size methods are less sensitive to changes in step size, and it is around a factor of 2 lower for AutoStep HMC and AutoStep MALA compared to methods with a fixed step size. This is because the AutoStep methods require multiple evaluations of the gradient during each iteration, which increases the computational cost. Despite this, the AutoStep methods give reliable performance without the need for manual tuning. On the challenging mRNA transfection problem, MALA fails when the step size is increased to 10 times the tuned value due to a rejection rate close to one (see Appendix B.5 for an empirical validation).

## B.5 Acceptance probability of AutoStep and fixed-step-size methods

We compare the average acceptance probability of AutoStep methods and fixed-step-size methods. Fig. 7 shows the average acceptance probability for AutoStep and fixed-step-size methods on the same benchmark set described in Section 5.1. All samplers are run for 19 tuning rounds, and the average acceptance probabilities are collected from the final round. AutoStep methods consistently target a reasonable acceptance probability. Conversely, the acceptance probabilities for fixed-step-size methods are highly sensitive to changes in step size. Small step sizes lead to acceptance probabilities near one, and large step sizes lead to acceptance probabilities near zero. Specifically, MALA using  $10.0 \times \theta_0$  yields an acceptance probability of zero on the mRNA transfection problem.



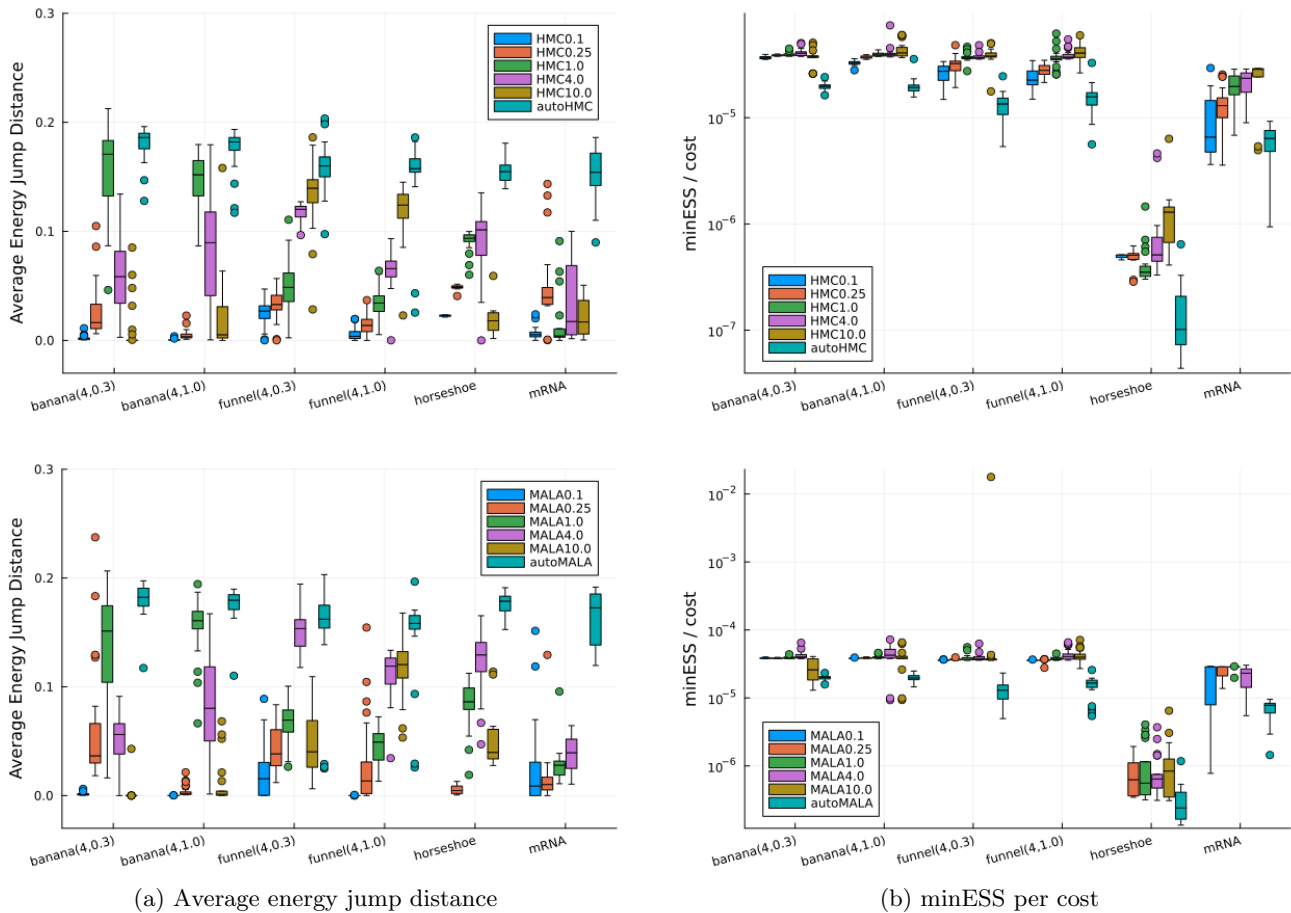


Figure 6: Average energy jump distance (left) and minESS per unit cost (right) for AutoStep HMC (top) and MALA (bottom). The fixed step sizes of the standard methods are set to  $\{0.1, 0.25, 1.0, 4.0, 10.0\} \times$  the tuned  $\theta_0$  from AutoStep methods.

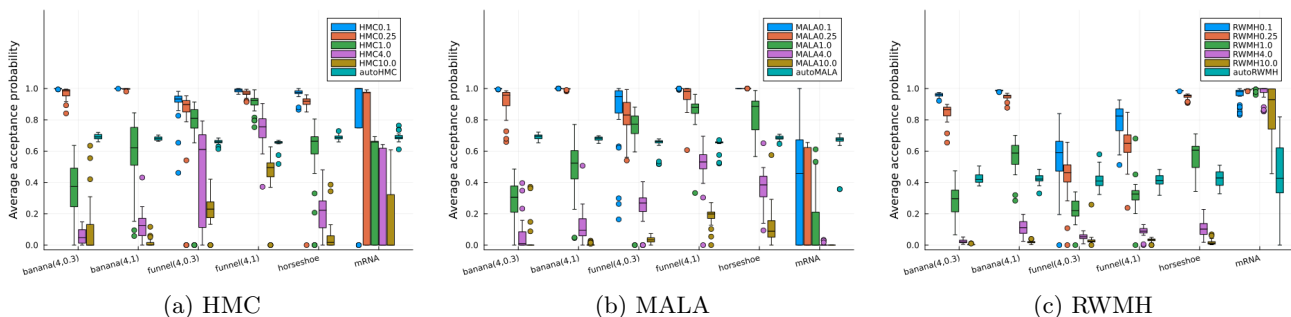


Figure 7: Average acceptance probabilities for HMC, MALA, and RWMH and their corresponding AutoStep methods across six models for the last tuning round. The fixed step sizes of the standard methods are set to  $\{0.1, 0.25, 1.0, 4.0, 10.0\} \times$  the tuned  $\theta_0$  from AutoStep methods.

### B.6 Comparing performance in terms of minESS per second (instead of unit cost)

In Section 5, we reported the experimental results in terms of minESS *per unit cost*. In this section, we present the same results expressed in terms of minESS *per second*. Fig. 8 (corresponds to Fig. 2 and Fig. 6) presents the minESS per second for both AutoStep and fixed-step-size methods. Despite the fact that AutoStep methods dynamically adjust the step size at each iteration, they consistently achieve minESS per second values that are comparable to those of the fixed-step-size methods. Fig. 9 (corresponds to Fig. 3) presents the effect of jitter and

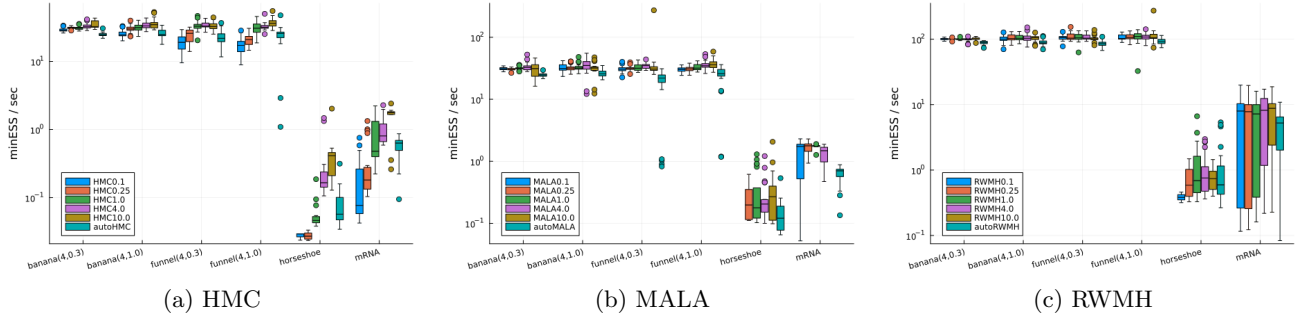


Figure 8: minESS per second for HMC, MALA, and RWMH and their corresponding AutoStep methods across six models. The fixed step sizes of the standard methods are set to  $\{0.1, 0.25, 1.0, 4.0, 10.0\} \times$  the tuned  $\theta_0$  from AutoStep methods.

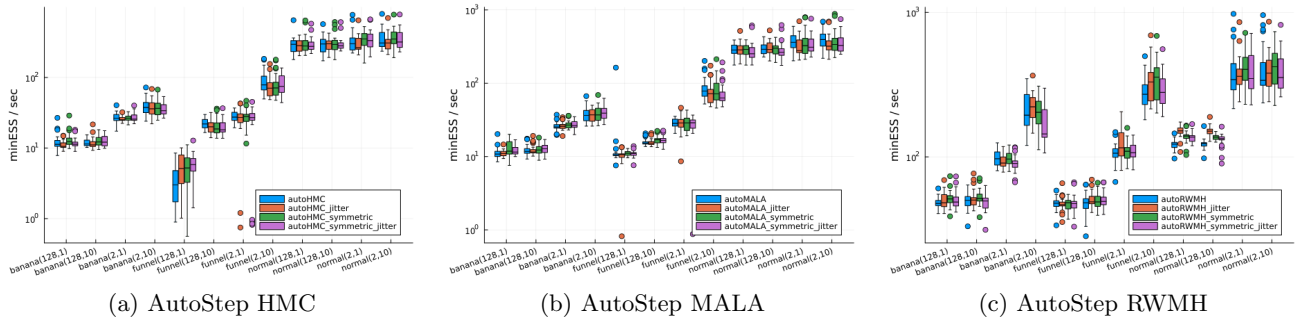


Figure 9: Comparison of each AutoStep MCMC method on the funnel, banana, and Gaussian distributions with varying dimensions and scales. The plots display the minESS per second for each method. We use the same model notation as in Fig. 3.

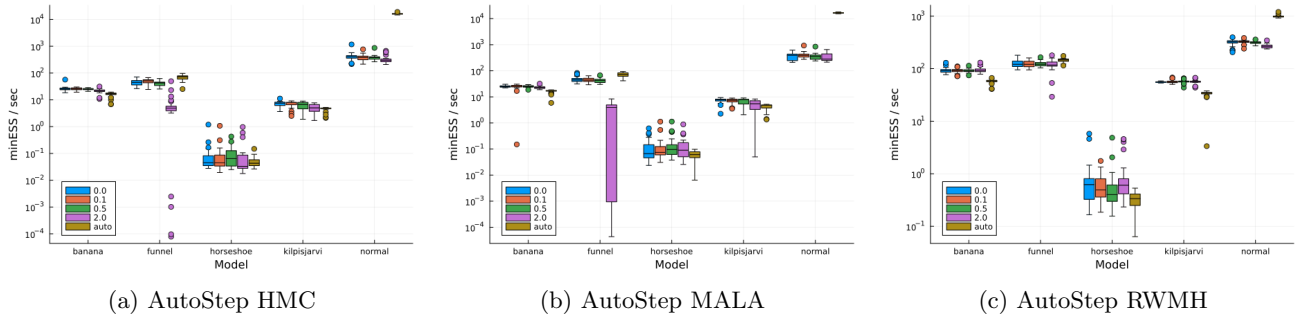


Figure 10: Comparison of auto-tuned jitter and fixed jitter for each AutoStep MCMC method. The plots display the minESS per second for each method. The legend distinguishes between the jitter tuning methods: “auto” represents auto-tuned jitter, and fixed jitter is denoted by a number, which corresponds to the jitter standard deviation  $\sigma$ .

the use of symmetric step size selector thresholds on minESS per second. It can be seen that the performance is consistent across all sampler variants. Fig. 10 (corresponds to Fig. 5) shows the effect of jitter tuning on the minESS per second for HMC, MALA and RWMH. The auto tuned jitter seems to provide consistently satisfactory performance. Notice that we use  $d = 2$  and  $\tau = 1$  for both the funnel and banana distributions.

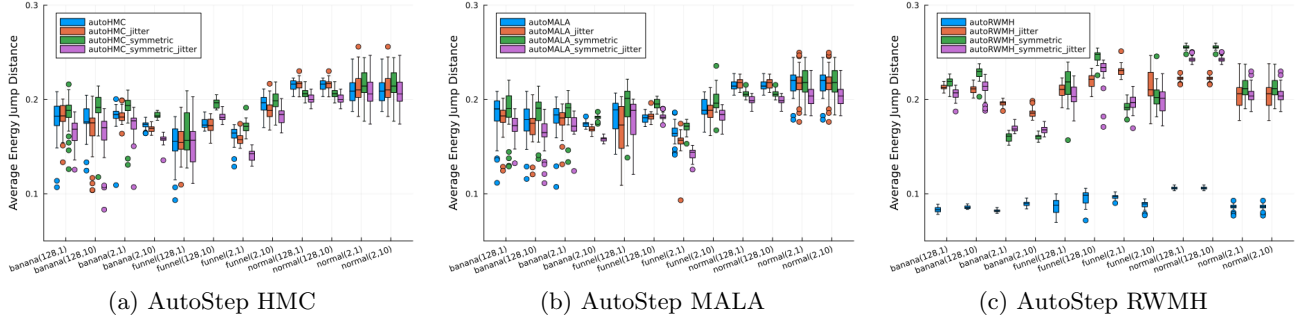


Figure 11: Comparison of each AutoStep MCMC method on the funnel, banana, and Gaussian distributions with varying dimensions and scales. The boxplots show the average energy jump distance. We use the same model notation as in Fig. 3.

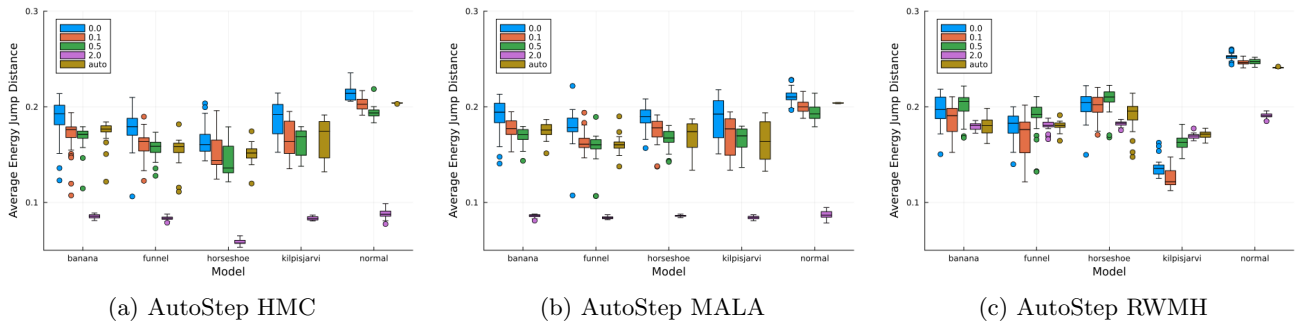


Figure 12: Comparison of auto-tuned jitter and fixed jitter for each AutoStep MCMC method. The boxplots show the average energy jump distance for the different variants of jitter. The legend distinguishes between the jitter tuning methods: “auto” represents auto-tuned jitter, and fixed jitter is denoted by a number, which corresponds to the jitter standard deviation  $\sigma$ .

## B.7 Effect of jitter and symmetric thresholds in terms of energy jump distance (instead of minESS)

In addition to the minESS, we report the average energy jump distance for each experiment mentioned in Section 5. Fig. 11 presents the effect of jitter and the use of symmetric step size selector thresholds on average energy jump distance. The performance is consistent across all sampler variants, except that RWMH benefits significantly by using symmetric thresholds and random jitter. Fig. 12 shows the effect of jitter tuning on average energy jump distance for AutoStep methods. The average energy jump distance appears to be sensitive to the jitter standard deviation, with larger  $\sigma$  generally leading to lower results. The auto tuned jitter method provides consistently satisfactory performance compared to well-tuned fixed jitter variants. As before, we use  $d = 2$  and  $\tau = 1$  for both the funnel and banana distributions.

## B.8 Comparison with existing adaptive samplers

We compare the performance of AutoStep methods to two existing state-of-the-art adaptive samplers: the No-U-Turn sampler (Hoffman and Gelman, 2014) from Turing.jl (Ge et al., 2018), and the hit-and-run slice sampler (Bélisle et al., 1993; Neal, 2003). For all AutoStep methods, we use symmetric acceptance thresholds and auto-tuned jitter as suggested in Section 5. The hit-and-run slice sampler uses univariate slice sampling (via doubling, as described in Figure 4 of Neal, 2003) within the hit-and-run algorithm. Concretely, at each point  $x$  with  $\pi(x) > 0$ , a direction  $z \sim \mathcal{N}(0, I)$  is sampled independently of other variables. Then, slice sampling is used to sample from the restriction of  $\pi$  to the line  $\{x + sz : s \in \mathbb{R}\}$  with initial point  $s = 0$ . The slicer uses an initial window size of 10 and a maximum number of 20 doublings. The sampler undergoes no adaptation in our round-based scheme. We simulate on six benchmark models, which include two funnels, two banana distributions, as well as the mRNA (Ballnus et al., 2017) and the logistic regression (Sejnowski and Gorman, 1988; Carvalho

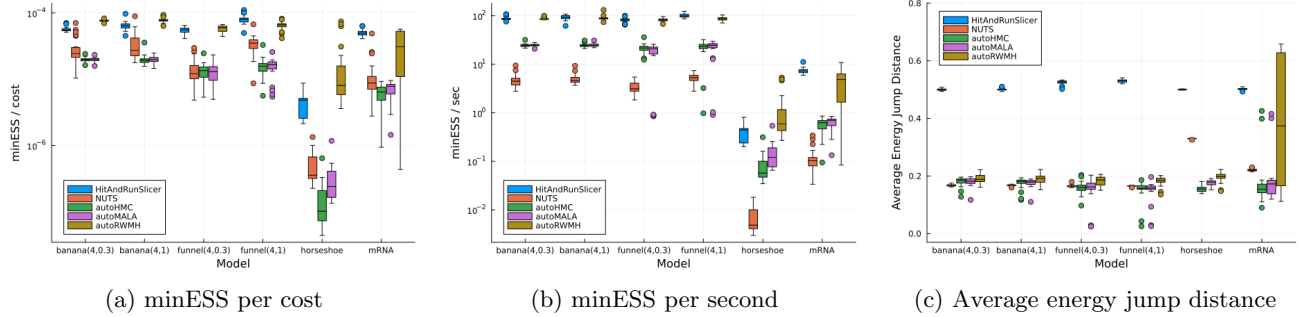


Figure 13: Performance comparison across six benchmarks for NUTS, the hit-and-run slice sampler, and three AutoStep methods.

et al., 2009) problems.

Fig. 13 demonstrates that AutoStep samplers generally offer competitive performance compared to both NUTS and the hit-and-run slice sampler in terms of minESS per unit cost and average energy jump distance. In terms of minESS per second, both AutoStep RWMH and the hit-and-run slice sampler offer fast sampling, whereas NUTS is significantly slower by comparison. However, we note that the minESS is not always a reliable measure of performance. For instance, although NUTS sometimes yields reasonable minESS values, it does not explore the sample space as effectively as the other methods. This is evident in Fig. 14, where we show pairplots of  $2^{17}$  samples generated by the five samplers on the mRNA problem. As seen in the figure, NUTS exhibits erratic behaviour compared to other methods. Furthermore, we should note that AutoStep RWMH shows greater variability in performance when applied to real data problems.

### B.9 Symmetric thresholds in AutoStep RWMH

We also empirically investigate the influence of symmetric thresholds when using AutoStep RWMH to ensure irreducibility. Fig. 1 illustrates a hypothetical scenario where AutoStep RWMH is applied to a 1D Gaussian distribution, which shows that symmetric thresholds help the sampler to explore modal regions. In support of Fig. 1, Fig. 15 displays the scatter plots for  $2^{13}$  samples obtained from AutoStep RWMH with and without symmetric thresholds applied to a 2D Gaussian distribution. Without symmetric thresholds, AutoStep RWMH rarely visits the mode of the distribution. However, AutoStep MALA and HMC with asymmetric thresholds do not experience this gap problem, because the use of an augmented space and projections onto the sample space mitigate the risk of overshooting.

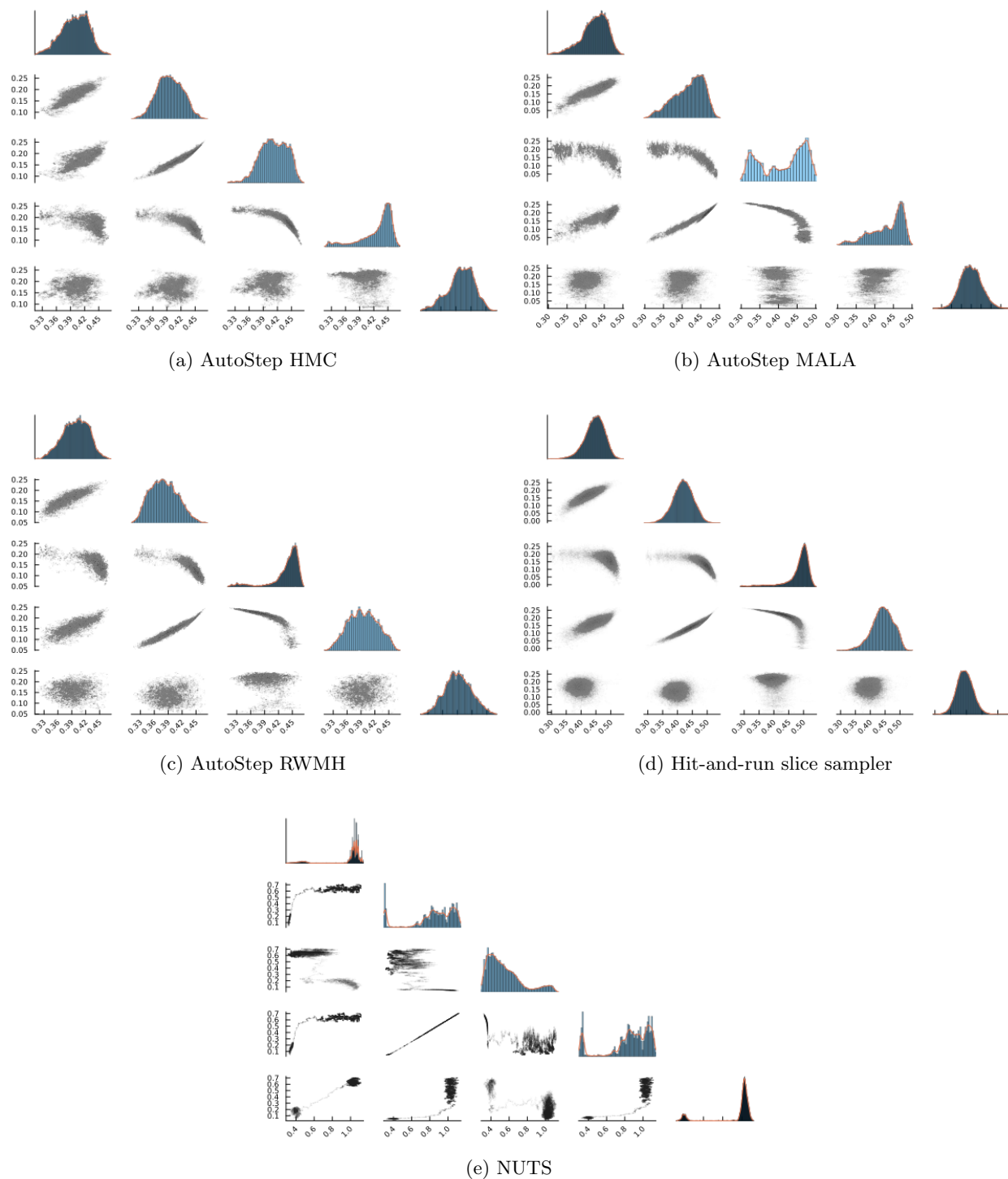


Figure 14: Pairplots of samples for different samplers on the mRNA model. Note that NUTS shows erratic behavior on this target when compared to other samplers.

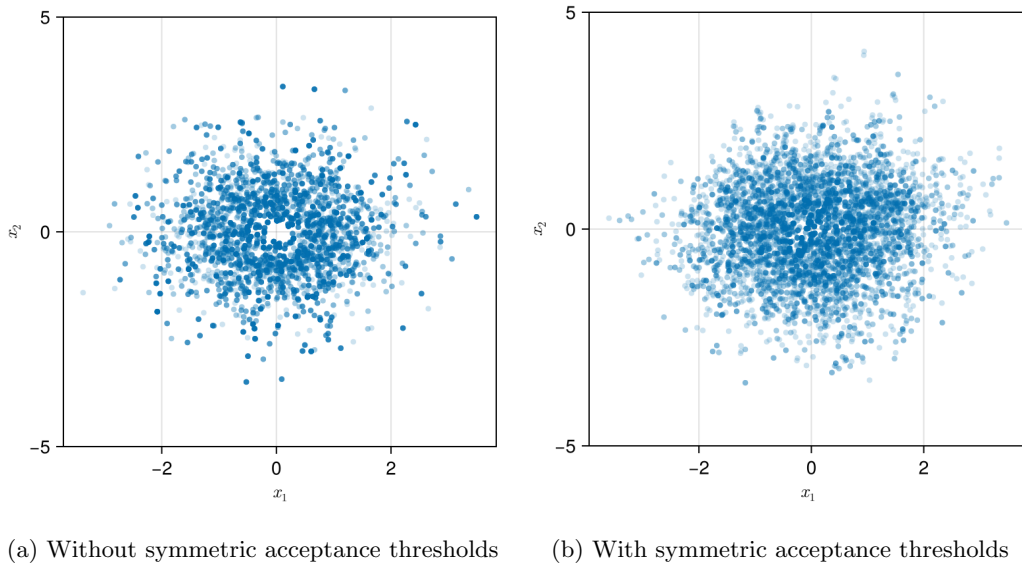


Figure 15: Scatter plots of samples obtained by AutoStep RWMH with no jitter on a 2D Gaussian target. Note that without the symmetric acceptance thresholds, there is a visible hole in the middle of the scatterplot for this target distribution.